hematopoietic stem cells (HSCs). Interestingly, among the four SFRP members, SFRP-1 and SFRP-2 were specifically induced in the bone marrow (BM) in response to myelosuppressive stimuli such as 5-fluorouracil (5-FU) or irradiation (Fig. 1A and B). In contrast, SFRP-3 and SFRP-4 were not expressed or constitutively expressed in the BM, and their expressions were not influenced by myelosuppression. These results suggest that SFRP-1 and SFRP-2 might be involved in the homeostasis of HSCs during myelosuppression.

SFRP-1 and SFRP-2 are expressed in osteoblasts

To elucidate where SFRP-1 and SFRP-2 are expressed in the BM, we performed immunostaining of the BM during myelosuppression. Interestingly, both proteins were constitutively expressed in osteoblasts (OBs), but not in hematopoietic cells (Fig. 1C and D). Under steady state conditions, OBs lined the surface of trabecular bones in metaphysis, but they were scarcely found in diaphysis (Fig. 1C and D). In contrast, 5-FU treatment increased the number of OBs in the diaphysis, whereas that in the metaphysis was unchanged. The expression of SFRP-1 or SFRP-2 in each osteoblast did not differ in the control or 5-FU-treated BM. These results suggest the increase of the number of OBs contributed to the up-regulation of SFRP-1 and SFRP-2 in the BM by 5-FU. Since OBs are one of the major components of the HSC niche, we speculated that SFRP-1 and SFRP-2 might regulate the HSC physiology under myelosuppression.

SFRP-1 and SFRP-2 stimulate proliferation of hematopoietic stem/progenitor cells, while they differentially affect their multilineage differentiation potential

Next, the effect of SFRP-1 and SFRP-2 on the growth and differentiation of HSCs was examined. $CD34^-c\text{-}Kit^+Sca\text{-}1^+lineage^-$ ($CD34^-KSL$) cells [23] were sorted from murine BM by flow cytometry (FACS) and subjected to an *in vitro* growth assay with or without SFRPs. As shown in Fig. 2A, both SFRP-1 and SFRP-2 stimulated the proliferation of $CD34^-KSL$ cells approximately 1.3–1.5-fold in comparison to the control-treated cells. This stimulatory effect for growth was more evident when SFRP-1 and SFRP-2 were overexpressed in $CD34^-KSL$ cells allowing autocrine production of the proteins (Fig. 2B). In this case, cellular proliferation was stimulated by approximately 2-fold by SFRP-2 and by 1.5-fold by SFRP-1.

Interestingly, colony assay revealed that the number of multipotent progenitors (MPPs; GEMM, and GEM in Fig. 3) generated from $CD34^-KSL$ cells decreased by approximately half by the treatment with SFRP-1 for 2-weeks. This indicates that SFRP-1 facilitates differentiation of $CD34^-KSL$ cells and many of the cells lose clonogenic potential during 2-weeks' culture. In sharp contrast, SFRP-2 slightly increased the number of MPPs (about 1.2-fold) in comparison to the controls by 2 weeks of culture (Fig. 3), showing that SFRP-2 preserves, or slightly enhances multilineage differentiation potential of $CD34^-KSL$ cells.

Taken together, while both SFRP-1 and SFRP-2 stimulate proliferation of $CD34^-KSL$ cells *in vitro*, they clearly differ in their ability to sustain multipotency of hematopoietic stem/progenitor cells.

SFRP-1 and SFRP-2 differentially regulate long-term repopulating potential of hematopoietic stem cells

Given that SFRP-1 and SFRP-2 affect the proliferation and differentiation potential of HSCs, they may also regulate the self-renewal and long-term repopulating (LTR) activities of HSCs. $CD34^-KSL$ cells were sorted by FACS, cultured *in vitro* with SFRP-1 or SFRP-2 for 2-weeks, and transplanted into lethally irradiated congenic recipient mice to assess their LTR activity. Surprisingly, HSCs treated with SFRP-1 almost completely lost their LTR activity, whereas those treated with SFRP-2 sustained that to a degree comparable to control-treated cells (Fig. 4A). Furthermore, the cells treated with SFRP-2 presented enhanced LTR potential in comparison to the controls in the secondary recipients (Fig. 4B), thus suggesting that SFRP-2 enhances self-renewal capacity of HSCs. These data show a clear difference between SFRP-1 and SFRP-2 in the regulation of LTR and self-renewal capacity of HSCs.

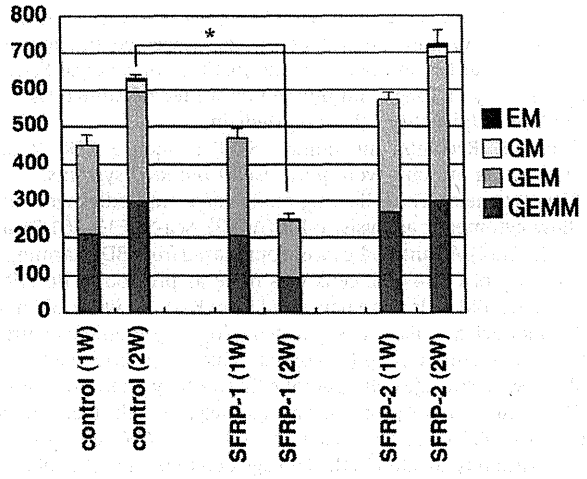

Fig. 3. Differential effects of SFRP-1 and SFRP-2 on the progenitor production by $CD34^-KSL$ cells. Fifty $CD34^-KSL$ cells were cultured in S-Clone SF-03 supplemented with 0.5% BSA, 50 μM 2-ME, SCF (50 ng/ml) and TPO (50 ng/ml) with SFRP-1 (1 μg/ml) or SFRP-2 (1 μg/ml) for 1 or 2 weeks, after which cells were subjected to colony assays. GEMM, granulocyte/erythroid/macrophage/megakaryocyte; GEM, granulocyte/erythroid/macrophage; GM, granulocyte/macrophage; EM, erythroid/megakaryocyte. Data are means ± S.D. ($n = 3$). $^*p < 0.05$.

Discussion

Although Wnt family proteins are well-known regulators of HSCs [2], the regulation of their activities remains obscure. This study showed that endogenous Wnt modulators, SFRP-1 and SFRP-2 are expressed in osteoblasts and they differentially affect the HSC activities. These findings raise a possibility that SFRP-1 and SFRP-2 play critical roles in regulating Wnt activities in the osteoblastic niche in the BM.

A previous study using drosophila Wnt and human SFRP-1 suggested that SFRPs act either positively or negatively on Wnt signaling depending on their concentration [11]. However, we observed that both human SFRP-1 and mouse SFRP-2 equally repressed mouse Wnt3a activity *in vitro* regardless of their concentration (Supplementary Fig. 1). Based on this observation, we speculated that both SFRP-1 and SFRP-2 act as negative regulators for Wnt signaling. However, our study revealed that, while both SFRP-1 and SFRP-2 enhanced the proliferation of $CD34^-KSL$ cells, they affected their clonogenicity and the LTR activity in a completely different manner at least *in vitro*.

In the colony assays, SFRP-1 reduced the number of mix colonies (GEMM and GEM) derived from $CD34^-KSL$ cells after 2-weeks of culture, while SFRP-2 enhanced it by approximately 1.2-fold. These data indicate that SFRP-1 facilitated differentiation of $CD34^-KSL$ cells so that many of the cells passed the stage of MPPs, leading to the decrease of mix colonies. In contrast, SFRP-2 enhanced the proliferation of $CD34^-KSL$ cells and increased the number of MPPs, suggesting that SFRP-2 stimulates proliferation of hematopoietic stem/progenitor cells with their multipotency being preserved.

The differential effect of SFRP-1 and SFRP-2 on the LTR capacity of HSCs was even more striking. By the treatment of $CD34^-KSL$

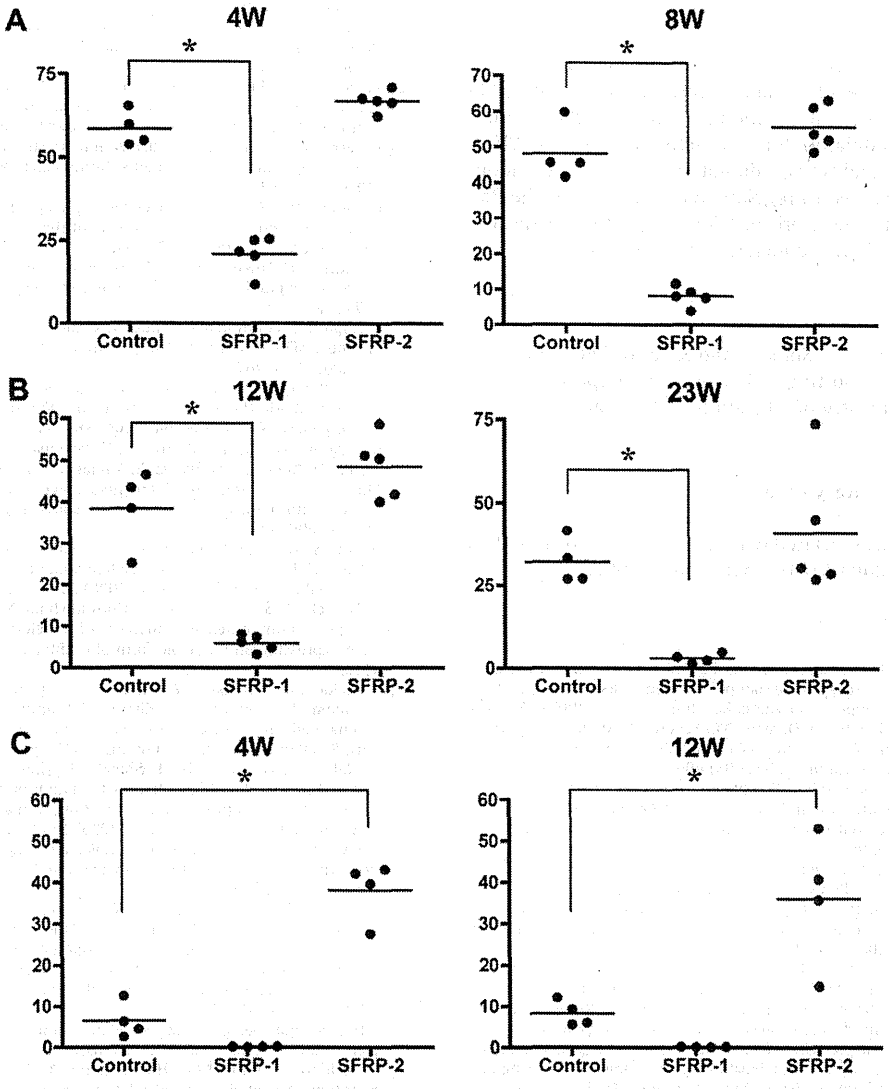

Fig. 4. Differential effects of SFRP-1 and SFRP-2 on the long-term repopulating capacity of $CD34^-KSL$ cells. (A) Long-term repopulating activity of $CD34^-KSL$ cells cultured with SFRP-1 or SFRP-2. Twenty $CD34^-KSL$ cells (Ly5.1) were cultured for 2 weeks in S-Clone SF-03 supplemented with 0.5% BSA, 50 μM 2-ME, 50 ng/ml SCF and 50 ng/ml TPO with SFRP-1 (1 μg/ml) or SFRP-2 (1 μg/ml). After the culture, cells were harvested and transplanted into lethally irradiated congenic hosts (Ly5.2) with 2×10^5 competitors (Ly5.2). Percentages of donor cells in peripheral blood were analyzed at the indicated time points. The data were not statistically different between the control- ($n = 4$) and SFRP-2-treated ($n = 5$) groups at any time points. In contrast, the control- and SFRP-1-treated groups were statistically different at all time points ($^*p < 0.05$). (B) Secondary transplantation. Bone marrow cells taken from the primary recipient mice shown in (A) were pooled and used for the secondary transplantation as described in the Materials and methods. The percentages of donor cells in peripheral blood were analyzed at the indicated time points ($n = 4$, $^*p < 0.05$).

cells with SFRP-1 for 2 weeks completely impaired their LTR capacity. In clear contrast, SFRP-2 enhanced the LTR activity of HSCs as revealed by the secondary transplantation. These observations are compatible with the adverse or positive effect of SFRP-1 or SFRP-2, respectively, on the multipotency of HSCs in the colony assays. Considering a role of Wnts in the self-renewal of HSCs, this study suggests that SFRP-1 and SFRP-2 may act as an antagonist and an agonist for Wnt signaling, respectively. Differential effects of SFRP-1 and SFRP-2 like this case have actually been reported previously in the apoptotic process of cancers and developmental patterning [24–26]. In addition, Yoshino et al. have suggested SFRP-2 did not inhibit Wnt signaling during metanephric kidney development, supporting our hypothesis of agonistic function of SFRP-2 on Wnt activity [27]. It is therefore plausible that SFRP proteins are context-dependent modulators for Wnt signaling and different SFRPs have distinct functions. Molecular basis for these differences is not clear yet, however, it is suggested that some SFRPs inhibit other SFRP function, or they may activate Fz receptors through direct binding [28].

One puzzling finding is SFRP-1 and SFRP-2 are simultaneously expressed in the osteoblasts in the BM. In this respect, different time courses of induction for both proteins (Fig. 1A) may give us a clue how these proteins play roles during myelosuppression. SFRP-1 is strongly induced in response to 5-FU on day 3, and its expression is sustained until day 9. In contrast, SFRP-2 is being turned on from day 3 to day 6, and is abruptly shut down on day 9. These different patterns of expression predict that SFRP-1 facilitates progenitor differentiation throughout the period of myelosuppression to supply mature hematopoietic cells, while SFRP-2 transiently stimulates self-renewing cell division of HSCs to provide MPPs for further differentiation and expansion. Irrespective, precise roles of SFRP-1 and SFRP-2 *in vivo* remain to be determined in the future study.

Conclusion

In conclusion, we revealed that SFRP-1 and SFRP-2 are expressed in the BM osteoblasts and differentially regulate HSC/progenitor functions *in vitro*. In addition to SFRPs, there are a number of endogenous modulators for Wnt activities such as WIF-1, Cerberus, and Dkk [5], and we still do not know how these modulators are integrated *in vivo* to regulate Wnt activities in the BM. Revealing the molecular network of Wnt modulators in the BM niche will enable us to better understand HSC regulation.

Acknowledgments

We thank N. Watanabe, T. Shibata, and S. Saito (FACS Core Laboratory, IMSUT) for FACS sorting. This work was supported in part by a grant from the Ministry of Education, Science, and Culture of Japan.

Appendix A. Supplementary data

Supplementary data associated with this article can be found, in the online version, at doi:10.1016/j.bbrc.2009.09.067.

References

[1] M. Kondo, A.J. Wagers, M.G. Manz, S.S. Prohaska, D.C. Scherer, G.F. Beilhack, J.A. Shizuru, I.L. Weissman, Biology of hematopoietic stem cells and progenitors: implications for clinical application, Annu. Rev. Immunol. 21 (2003) 759–806.
[2] T. Reya, A.W. Duncan, L. Ailles, J. Domen, D.C. Scherer, K. Willert, L. Hintz, R. Nusse, I.L. Weissman, A role for Wnt signalling in self-renewal of haematopoietic stem cells, Nature 423 (2003) 409–414.
[3] R. Nusse, Wnt signaling and stem cell control, Cell Res. 18 (2008) 523–527.
[4] R. Nusse, Wnt signaling in disease and in development, Cell Res. 15 (2005) 28–32.
[5] Y. Kawano, R. Kypta, Secreted antagonists of the Wnt signalling pathway, J. Cell Sci. 116 (2003) 2627–2634.
[6] S.E. Jones, C. Jomary, Secreted Frizzled-related proteins: searching for relationships and patterns, Bioessays 24 (2002) 811–820.
[7] C.E. Dann, J.C. Hsieh, A. Rattner, D. Sharma, J. Nathans, D.J. Leahy, Insights into Wnt binding and signalling from the structures of two Frizzled cysteine-rich domains, Nature 412 (2001) 86–90.
[8] H. Suzuki, D.N. Watkins, K.W. Jair, K.E. Schuebel, S.D. Markowitz, W.D. Chen, T.P. Pretlow, B. Yang, Y. Akiyama, M. Van Engeland, M. Toyota, T. Tokino, Y. Hinoda, K. Imai, J.G. Herman, S.B. Baylin, Epigenetic inactivation of SFRP genes allows constitutive WNT signaling in colorectal cancer, Nat. Genet. 36 (2004) 417–422.
[9] P.W. Finch, X. He, M.J. Kelley, A. Uren, R.P. Schaudies, N.C. Popescu, S. Rudikoff, S.A. Aaronson, H.E. Varmus, J.S. Rubin, Purification and molecular cloning of a secreted, Frizzled-related antagonist of Wnt action, Proc. Natl. Acad. Sci. USA 94 (1997) 6770–6775.
[10] S. Dennis, M. Aikawa, W. Szeto, P.A. d'Amore, J. Papkoff, A secreted frizzled related protein, FrzA, selectively associates with Wnt-1 protein and regulates wnt-1 signaling, J. Cell Sci. 112 (Pt 21) (1999) 3815–3820.
[11] A. Uren, F. Reichsman, V. Anest, W.G. Taylor, K. Muraiso, D.P. Bottaro, S. Cumberledge, J.S. Rubin, Secreted frizzled-related protein-1 binds directly to Wingless and is a biphasic modulator of Wnt signaling, J. Biol. Chem. 275 (2000) 4374–4382.
[12] W. Satoh, M. Matsuyama, H. Takemura, S. Aizawa, A. Shimono, Sfrp1, Sfrp2, and Sfrp5 regulate the Wnt/beta-catenin and the planar cell polarity pathways during early trunk formation in mouse, Genesis 46 (2008) 92–103.
[13] K. Terry, H. Magan, M. Baranski, L.W. Burrus, Sfrp-1 and sfrp-2 are expressed in overlapping and distinct domains during chick development, Mech. Dev. 97 (2000) 177–182.
[14] C. Leimeister, A. Bach, M. Gessler, Developmental expression patterns of mouse sFRP genes encoding members of the secreted frizzled related protein family, Mech. Dev. 75 (1998) 29–42.
[15] A.S. Kim, D.H. Lowenstein, S.J. Pleasure, Wnt receptors and Wnt inhibitors are expressed in gradients in the developing telencephalon, Mech. Dev. 103 (2001) 167–172.
[16] B. Jaspard, T. Couffinhal, P. Dufourcq, C. Moreau, C. Duplaa, Expression pattern of mouse sFRP-1 and mWnt-8 gene during heart morphogenesis, Mech. Dev. 90 (2000) 263–267.
[17] G.M. Caldwell, C. Jones, K. Gensberg, S. Jan, R.G. Hardy, P. Byrd, S. Chughtai, Y. Wallis, G.M. Matthews, D.G. Morton, The Wnt antagonist sFRP1 in colorectal tumorigenesis, Cancer Res. 64 (2004) 883–888.
[18] M. Nojima, H. Suzuki, M. Toyota, Y. Watanabe, R. Maruyama, S. Sasaki, Y. Sasaki, H. Mita, N. Nishikawa, K. Yamaguchi, K. Hirata, F. Itoh, T. Tokino, M. Mori, K. Imai, Y. Shinomura, Frequent epigenetic inactivation of SFRP genes and constitutive activation of Wnt signaling in gastric cancer, Oncogene 26 (2007) 4699–4713.
[19] H. Ema, Y. Morita, S. Yamazaki, A. Matsubara, J. Seita, Y. Tadokoro, H. Kondo, H. Takano, H. Nakauchi, Adult mouse hematopoietic stem cells: purification and single-cell assays, Nat. Protoc. 1 (2006) 2979–2987.
[20] Y. Fukuchi, F. Shibata, M. Ito, Y. Goto-Koshino, Y. Sotomaru, T. Kitamura, H. Nakajima, Comprehensive analysis of myeloid lineage conversion using mice expressing an inducible form of C/EBP alpha, EMBO J. 25 (2006) 3398–3410.
[21] H. Nakajima, F. Shibata, Y. Fukuchi, Y. Goto-Koshino, M. Ito, A. Urano, T. Nakahata, H. Aburatani, T. Kitamura, Immune suppressor factor confers stromal cell line with enhanced supporting activity for hematopoietic stem cells, Biochem. Biophys. Res. Commun. 340 (2006) 35–42.
[22] H. Nakajima, N. Watanabe, F. Shibata, T. Kitamura, Y. Ikeda, M. Handa, N-terminal region of CCAAT/enhancer binding protein epsilon is critical for cell cycle arrest, apoptosis and functional maturation during myeloid differentiation, J. Biol. Chem. 281 (2006) 14494–14502.
[23] M. Osawa, K. Hanada, H. Hamada, H. Nakauchi, Long-term lymphohematopoietic reconstitution by a single CD34-low/negative hematopoietic stem cell, Science 273 (1996) 242–245.
[24] H.S. Melkonyan, W.C. Chang, J.P. Shapiro, M. Mahadevappa, P.A. Fitzpatrick, M.C. Kiefer, L.D. Tomei, S.R. Umansky, SARPs: a family of secreted apoptosis-related proteins, Proc. Natl. Acad. Sci. USA 94 (1997) 13636–13641.
[25] D.L. Ellies, V. Church, P. Francis-West, A. Lumsden, The WNT antagonist cSFRP2 modulates programmed cell death in the developing hindbrain, Development 127 (2000) 5285–5295.
[26] X. Han, S. Amar, Secreted frizzled-related protein 1 (SFRP1) protects fibroblasts from ceramide-induced apoptosis, J. Biol. Chem. 279 (2004) 2832–2840.
[27] K. Yoshino, J.S. Rubin, K.G. Higinbotham, A. Uren, V. Anest, S.Y. Plisov, A.O. Perantoni, Secreted Frizzled-related proteins can regulate metanephric development, Mech. Dev. 102 (2001) 45–55.
[28] P. Bovolenta, P. Esteve, J.M. Ruiz, E. Cisneros, J. Lopez-Rios, Beyond Wnt inhibition: new functions of secreted Frizzled-related proteins in development and disease, J. Cell Sci. 121 (2008) 737–746.

THE JOURNAL OF BIOLOGICAL CHEMISTRY VOL. 284, NO. 45, pp. 31463–31472, November 6, 2009

Evidence That Integrin αIIbβ3-dependent Interaction of Mast Cells with Fibrinogen Exacerbates Chronic Inflammation*

Received for publication, June 6, 2009, and in revised form, July 22, 2009 Published, JBC Papers in Press, September 15, 2009, DOI 10.1074/jbc.M109.030213

Toshihiko Oki[‡], Koji Eto[§], Kumi Izawa[‡], Yoshinori Yamanishi[‡], Naoki Inagaki[¶], Jon Frampton[‖], Toshio Kitamura[‡], and Jiro Kitaura[‡1]

From the [‡]Division of Cellular Therapy, Advanced Clinical Research Center, The Institute of Medical Science, The University of Tokyo, 4-6-1 Shirokanedai, Minato-ku, Tokyo 108-8639, Japan, the [§]Division of Stem Cell Therapy, Center for Stem Cell and Regenerative Medicine, The Institute of Medical Science, University of Tokyo, Tokyo 108-8639, Japan, the [¶]Department of Pharmacology, Gifu Pharmaceutical University, Gifu 502-8585, Japan, and the [‖]Division of Immunity and Infection, Medical Research Council Centre for Immune Regulation, University of Birmingham, Birmingham B15 2TT, United Kingdom

Integrin αIIbβ3 is expressed in mast cells as well as in megakaryocytes/platelets. A recent study has shown that surface expression levels of integrin αVβ3 are elevated in integrin αIIb-deficient bone marrow-derived mast cells (BMMCs) as compared with wild-type (WT) counterparts, but the underlying mechanism remains obscure. Here we demonstrate by transducing integrin αIIb into integrin αIIb-deficient BMMCs that surface expression levels of integrin αVβ3 are inversely related to those of integrin αIIbβ3. Thus, competitive association of integrin β3 with integrin αIIb or integrin αV determines surface expression levels of integrin αIIbβ3 or αVβ3 in mast cells. We compared WT and integrin αIIb-deficient BMMCs as well as integrin αIIb-deficient BMMCs transduced with integrin αIIb(WT) or non-functional αIIb(D163A) mutant and found that enhancement of proliferation, degranulation, cytokine production, and migration of BMMCs through interaction with fibrinogen (FB) depended on integrin αIIbβ3. In addition, elevated surface expression of integrin αVβ3 failed to compensate for loss of FB-associated functions in integrin αIIb-deficient BMMCs while enhancing adhesion to vitronectin or von Willebrand factor. Importantly, integrin αIIb deficiency strongly suppressed chronic inflammation with the remarkable increase of mast cells induced by continuous intraperitoneal administration of FB, although it did not affect acute allergic responses or mast cell numbers in tissues in steady states. Interestingly, soluble FB promoted cytokine production of BMMCs in response to *Staphylococcus aureus* with FB-binding capacity, through integrin αIIbβ3-dependent recognition of this pathogen. Collectively, integrin αIIbβ3 in mast cells plays an important part in FB-associated, chronic inflammation and innate immune responses.

Mast cells play a critical role in IgE-associated allergic disorders, but recent advances have delineated the involvement of mast cells in IgE-independent physiological and pathological processes, including certain innate immune responses. In fact, various stimuli, in addition to IgE and specific antigens, can activate mast cells to release a diverse array of preformed and newly synthesized pro-inflammatory mediators such as histamine, lipids, cytokines, and chemokines (1–4). Although mast cell numbers and activation in tissues are closely related to mast cell-mediated immunity, the underlying mechanism remains incompletely understood. As one of the key phenomena, mast cells interact with the extracellular matrix (ECM)[2] through integrins composed of two subunits (α and β), thereby regulating mast cell functions. As previously reported (5–9), integrins α4β1 and α5β1, or integrin αVβ3, expressed in mast cells mediate binding to fibronectin (FN) or vitronectin (VN), respectively. Interestingly, integrin α4β7 is involved in intestinal homing of mast cell progenitors via interaction with mucosal vascular addressin cell adhesion molecule-1 (10). In view of the implication of mast cell integrins in innate immunity, integrin α2β1 expressed in peritoneal mast cells is required for the induction of inflammatory responses to infection (11). In addition, integrin αVβ6 is essential for nematode-induced mucosal mast cell hyperplasia and for expression of the granule chymase (12).

Integrin αIIb, also known as CD41, which forms a complex with integrin β3, is a well known marker of the megakaryocyte/platelet lineage. Integrin αIIbβ3 is required for normal platelet hemostatic function (13–17). Previously, we reported that integrin αIIbβ3 is also highly expressed in mast cells (9, 18). In addition, we demonstrated that mast cell interaction with fibrinogen (FB) via integrin αIIbβ3 enhances *in vitro* mast cell functions, by using a blocking Ab specific for integrin αIIb (9). On the other hand, higher surface expression levels of integrin αV and enhanced adhesion to VN were found in integrin αIIb-deficient BMMCs as compared with wild-type (WT) counterparts (18), suggesting that integrin αIIb and integrin αV counter-regulate their surface expression levels and functions in mast cells. Therefore, we attempted to carefully analyze the regulatory mechanisms by utilizing retroviral transduction with integrin αIIb WT or non-functional mutant into integrin αIIb-deficient BMMCs.

* This work was supported by grants from the Ministry of Education, Science, Technology, Sports and Culture and the Ministry of Health and Welfare, Japan.

[1] To whom correspondence should be addressed. Tel.: 81-3-5449-5759; Fax: 81-3-5449-5428; E-mail: kitaura-tky@umin.ac.jp.

[2] The abbreviations used are: ECM, extracellular matrix; BMMCs, bone marrow-derived mast cells; FB, fibrinogen; FN, fibronectin; SA, fixed *S. aureus* Cowan I; PCA, passive cutaneous allergic reaction; SCF, stem cell factor; VN, vitronectin; vWF, von Willebrand factor; WT, wild type; Ab, antibody; mAb, monoclonal antibody; IL-3, interleukin-3; BSA, bovine serum albumin; PBS, phosphate-buffered saline; LPS, lipopolysaccharide; TNP, trinitrophenol; DNP, dinitrophenol; WT, wild type; KO, knockout.

FB abundant in plasma contributes to blood clotting (19). In addition, FB as well as its degradation product fibrin are also present in ECM outside blood vessels, where they play important roles in inflammation and wound healing through recruitment and activation of inflammatory cells expressing FB-binding receptors (19–22). Interestingly, surface proteins that bind to FB are also expressed by several types of bacteria, such as *Staphylococcus aureus* and *Streptococcus pyogenes*, which modulate immune responses to bacterial infections (23–25).

In the present study, we showed that integrin αIIb expression levels regulate surface expression levels of integrin αVβ3 as well as integrin αIIbβ3 in mast cells and that mast cell functions augmented by interaction with FB are dependent on integrin αIIbβ3 and independent of integrin αVβ3. In accordance, integrin αIIb deficiency strongly suppressed FB-induced chronic inflammation. Notably, the interaction with soluble FB via integrin αIIbβ3 helps mast cells recognize and respond to *S. aureus* (Cowan I) with FB-binding capacity. Thus, integrin αIIbβ3 in mast cells modulates FB-associated, chronic inflammation and innate immune responses.

EXPERIMENTAL PROCEDURES

Mice—All experimental mice were sex- and age-matched (6–16 weeks old). Balb/c mice were purchased from Charles River Japan (Tokyo, Japan). Integrin aIIb$^{-/-}$ mice were generated as described previously (14) and backcrossed to Balb/c mice for at least six generations. Animal studies were performed according to the guidelines of the animal care committee of the Institute of Medical Science, University of Tokyo.

Antibodies and Other Materials—Source of antibodies (Abs) were as follows: anti-mouse integrin αIIbβ3 mAb (1B5) was a kind gift from Dr. B. S. Coller (Rockefeller University, New York, NY) (26). Anti-mouse integrin αV (8B3) and anti-mouse integrin β3 (8B11) mAbs were kind gifts from Drs. D. J. Gerber and S. Tonegawa (Picower Center, Massachusetts Institute of Technology, Boston, MA) (27). Anti-dinitrophenol (DNP) IgE (SPE-7) was from Sigma. Anti-trinitrophenol (TNP) IgE (C38-2), anti-mouse αIIb (MWReg30), anti-mouse αV (RMV-7 and H9.2B8), anti-mouse α4 (9C10), anti-mouse α5 (5H10–27), anti-mouse LFA1 (M17/4), anti-mouse β1 (Ha2/5), anti-mouse β2 (GAME-46), and anti-αVβ3 (2C9.G2) mAbs and other Abs were from BD Pharmingen. Cytokines such as mouse IL-3 and SCF were obtained from R&D Systems. Bovine serum VN and TNP-conjugated BSA (TNP-BSA) were from Sigma. Human plasma FB and von Willebrand factor (vWF) were from Chemicon. Formalin-fixed *S. aureus* Cowan I was purchased from Calbiochem.

Cells—To generate BMMCs with 95% purity (c-kit$^+$/FcεRI$^+$ by flow cytometry), bone marrow cells from 6-week-old male mice were cultured for 5–8 weeks in the presence of 10 ng/ml IL-3 with or without 20 ng/ml SCF as described previously (9, 28).

DNA Constructs, Transfection, and Infection—To generate mouse integrin αIIb(D163A) mutant, two-step PCR mutagenesis was performed by using mouse integrin αIIb wild-type (WT) cDNA (provided by Dr. R. B. Basani, Children's Hospital of Philadelphia, PA) as a template. Retroviral transfection was as described in a previous study (29). Briefly, integrin αIIb(WT) or αIIb(D163A) mutant cDNA was subcloned into pMXs-IRES-puro^r (pMXs-IP) to generate pMXs-IP-integrin αIIb(WT) or αIIb(D163A), respectively. To generate recombinant retroviruses, pMXs-IP plasmids were transfected into PLAT-E packaging cells (30) with FuGENE 6 (Roche Diagnostics). Cells were infected with retroviruses in the presence of 10 μg/ml Polybrene. Selection with puromycin was started 48 h after infection.

Flow Cytometric Analysis—Cells were stained as described before (9, 28). Cells stained with the indicated Abs were analyzed with a FACSCalibur equipped with CellQuest software (BD Biosciences) and Flowjo software (Tree Star).

Adhesion Assay and Migration Assay—Adhesion assay was done as described (6, 9). In brief, 96-well plates were coated with 20 μg/ml FB, FN, VN, or vWF. BMMCs resuspended at 5×10^5 cells/ml were transferred into coated wells with or without stimulant for 1 h at 37 °C. After washing, cell adhesion was quantitated using CellTiter-Glo™ (Promega, Madison, WI) and a Micro Lumat Plus luminometer (EG&G Berthold), according to the manufacturer's instructions. In assays using blocking Abs, BMMCs were preincubated with 20 μg/ml Abs for 1 h before adding the cells to the plate. Migration assays were carried out as described (7, 9), using 24-well Transwell chambers with 5-μm polycarbonate filters (Corning).

Measurement of Cytokines—The cells were transferred into FB-coated 96-well plates (1×10^4 cells/well) with or without stimulants. After incubating for 12 h at 37 °C, the supernatant of each well was collected, and the concentration of IL-6 or TNF-α was quantified by enzyme-linked immunosorbent assay with OptiEIA for IL-6 or TNF-α (BD Pharmingen) as described (9, 28).

β-Hexosaminidase Release Assay—β-Hexosaminidase release assay was as described before (31). Briefly, 5×10^4 cells of IgE-sensitized BMMCs in Tyrode buffer (10 mM HEPES buffer (pH 7.4), 130 mM NaCl, 5 mM KCl, and 5.6 mM glucose) containing 0.1% BSA, 1 mM $CaCl_2$, and 0.5 mM $MgCl_2$ were stimulated with the indicated concentration of TNP-BSA in BSA- or FB-coated 96-well plates for 1 h at 37 °C. Cell supernatants and total cell lysates solubilized with 1% Nonidet P-40 were collected, and β-hexosaminidase in the supernatants and cell lysates was quantified by spectrophotometric analysis of hydrolysis of *p*-nitrophenyl-*N*-acetyl-β-D-glucopyranoside (Sigma). The percentage of β-hexosaminidase release was calculated.

PCA Reactions—Passive cutaneous anaphylactic (PCA) reactions were performed as described (32–34). Briefly, anti-DNP IgE was intradermally injected into the ears of mice. After 24 h, 250 μg of DNP-BSA and 0.5% Evans blue dye was intravenously injected. The amounts of extravasated dye were measured after 30 min by extracting ears. In another type of experiment, mice received anti-DNP IgE intravenously. After 24 h, a skin reaction was elicited by applying 0.75% dinitrofluorobenzene acetone-olive oil solution to both sides of the ears. The reaction was assessed by measuring the ear thickness 1 h and 12 h after antigen challenge.

FB-induced Chronic Inflammation Model—200 μl of 0.5 mg/ml FB or PBS was intraperitoneally injected into WT or integrin αIIb$^{-/-}$ mice every 2 days. After 1 month, total peritoneal cells of the sacrificed mice were collected by using 3 ml of PBS. Total cell numbers were counted by using a hemocytometer; the percentages of mast cells (c-kit$^+$/FcεRI$^+$), granulo-

cytes (Gr-1^{high}/CD11b^{+}), and macrophages (F4/80^{+}) were calculated by fluorescence-activated cell sorting analysis.

Responses to Fixed S. aureus Cowan I in BMMCs—Fixed *S. aureus* Cowan I (SA) purchased from Calbiochem was stained with Cell Tracker Orange (Molecular Probes). Five × 10^4 BMMCs suspended in 10% BSA/Tyrode buffer were incubated with SA in the presence or absence of 0.5 mg/ml soluble FB in BSA-coated 96-well plates for 2 h. The interaction between mast cells and SA was observed by using a fluorescence microscope. After the supernatant of each well was collected, bacterial cells were removed with a 0.22-μm filter. Cytokine concentrations in the supernatants were quantified by enzyme-linked immunosorbent assay.

Quantitation of Tissue Mast Cells—Tissue mast cells in ear skin, back skin, peritoneal wall, and intestine were quantified by light microscopy at ×400 by an observer who was unaware of the identity (*i.e.* mouse genotype) of the individual specimens, in Giemsa-stained sections, as previously described (28, 35, 36). Results were expressed as mast cells (mean ± S.E.) per mm^2.

Statistical Analysis—Data are shown as the mean ± S.D. Statistical significance was determined by Student's *t* test, with $p < 0.01$ (**) and $p < 0.05$ (*) taken as being statistically significant.

RESULTS

Surface Expression Levels of Integrin αV Are Elevated in Integrin αIIb-deficient BMMCs—To investigate the role of integrin αIIb in mast cells, bone marrow cells from WT and integrin αIIb$^{-/-}$ mice were cultured in the presence of IL-3 for 5 weeks to generate comparable numbers of morphologically pure (>95%) mast cells. BMMCs from WT and integrin αIIb$^{-/-}$ Balb/c mice exhibited similar levels of FcεRI and c-kit on their cell surfaces as determined by flow cytometry (Fig. 1*A*). In addition, proliferative responses to IL-3 as well as apoptosis induced by growth factor (IL-3) deprivation were comparable between both BMMCs (Fig. 1, *C* and *D*). Thus, integrin αIIb deficiency did not affect Balb/c mice-derived mast cell development and growth in suspension culture, as previously reported in C57BL/6 mice (18). Moreover, when IgE-sensitized BMMCs were stimulated with the indicated doses of antigen, we found comparable levels of β-hexosaminidase release and cytokine (IL-6 and TNF-α) production (Fig. 1, *E* and *F*, and data not shown). This also suggested that integrin αIIb deficiency did not modulate FcεRI signaling in suspension culture of mast cells. However, in keeping with previous findings (18), we confirmed the striking differences between the two cell types: surface expression levels of integrin αV and integrin αVβ3 were 10-fold higher in integrin αIIb-deficient BMMCs as compared with WT counterparts, despite comparable expression levels of other integrins such as integrins α4, α5, and β1, and no detectable expression of integrin β2 in either BMMC (Fig. 1*E*). Collectively, these results led us to postulate that integrin αIIb deficiency influenced mast cell functions through interaction with ECM.

Surface Expression Levels of Integrin αV Are Inversely Correlated with Those of Integrin αIIb—We next investigated the mechanism by which surface expression levels of integrin αV were elevated in integrin αIIb-deficient BMMCs. As previously reported (18), mRNA levels of integrin αV and integrin β3 were comparable between WT and integrin αIIb-deficient BMMCs (data not shown), suggesting the post-translational regulation of surface expression levels of integrin αV in BMMCs. Because integrin β3 forms a complex with integrin αIIb or integrin αV, we hypothesized that integrin αV competed with integrin αIIb in the association with integrin β3. To test this, integrin αIIb-deficient BMMCs were retrovirally transduced with integrin αIIb WT or mock. Notably, flow cytometric analysis demonstrated that transduction with integrin αIIb(WT) strongly down-regulated surface expression of integrin αV in integrin αIIb-deficient BMMCs (Fig. 2*A*). In addition, integrin αIIb-(D163A) mutant (37), which lost the capacity to bind to FB, was transduced into integrin αIIb-deficient BMMCs. Consistent with a previous report (37), surface expression levels of integrin αIIb(D163A) mutant were weaker than those of integrin αIIb(WT) in the transduced cells. In proportion to less induction of integrin αIIb(D163A), surface expression levels of integrin αV in integrin αIIb(D163A) mutant-transduced cells were less down-regulated as compared with those in integrin αIIb(WT)-transduced BMMCs (Fig. 2*A*). Furthermore, similar experiments were performed using murine T cell lymphoma cell line BW5147, which originally expressed integrin αVβ3 but not integrin αIIbβ3. As shown in Fig. 2*B*, transduction with integrin αIIb(WT) into BW5147 cells down-regulated surface expression of integrin αV to a greater degree as compared with transduction with integrin αIIb(D163A) mutant. Collectively, surface expression levels of integrin αV were inversely related to those of integrin αIIb, and even non-functional integrin αIIb competed with integrin αV for integrin β3.

Reduced Adhesion to FB and Enhanced Adhesion to VN and vWF in Integrin αIIb-deficient BMMCs—Next, we examined the effects of integrin αIIb deficiency on mast-cell adhesion to ECM proteins such as FN, FB, VN, and vWF. IgE stimulation-dependent adhesion to FB was strongly suppressed in integrin αIIb-deficient BMMCs, whereas adhesion to VN or vWF was drastically enhanced in integrin αIIb-deficient BMMCs, presumably because of increased surface expression of integrin αVβ3 in integrin αIIb-deficient BMMCs when compared with WT BMMCs (Fig. 3*A*). On the other hand, integrin αIIb deficiency did not significantly affect the adhesion to FN (Fig. 3*A*). In addition, we examined the inhibitory effect of pretreatment with blocking Abs against integrin αIIbβ3 or integrin αVβ3 on mast-cell adhesion to ECM proteins, confirming that, in WT BMMCs, the binding to FB, VN, or vWF was dependent on integrin αIIbβ3, integrin αVβ3, or both (Fig. 3*B*). Similar experiments were also performed with regard to integrin αIIb-deficient BMMCs, demonstrating that pretreatment with blocking Abs against integrin αV dampened IgE stimulation-dependent strong adhesion to VN or vWF as well as weak adhesion to FB, whereas it did not affect the adhesion to FN (Fig. 3*B*). In contrast, pretreatment with blocking Ab for integrin αIIb did not reduce the adhesive property at all (Fig. 3*B*). Collectively, these results suggested that elevated surface expression levels of integrin αVβ3 in αIIb-deficient BMMCs enhanced the adhesion to VN or vWF, but it did not compensate for the defective adhesion to FB owing to integrin αIIbβ3 deficiency.

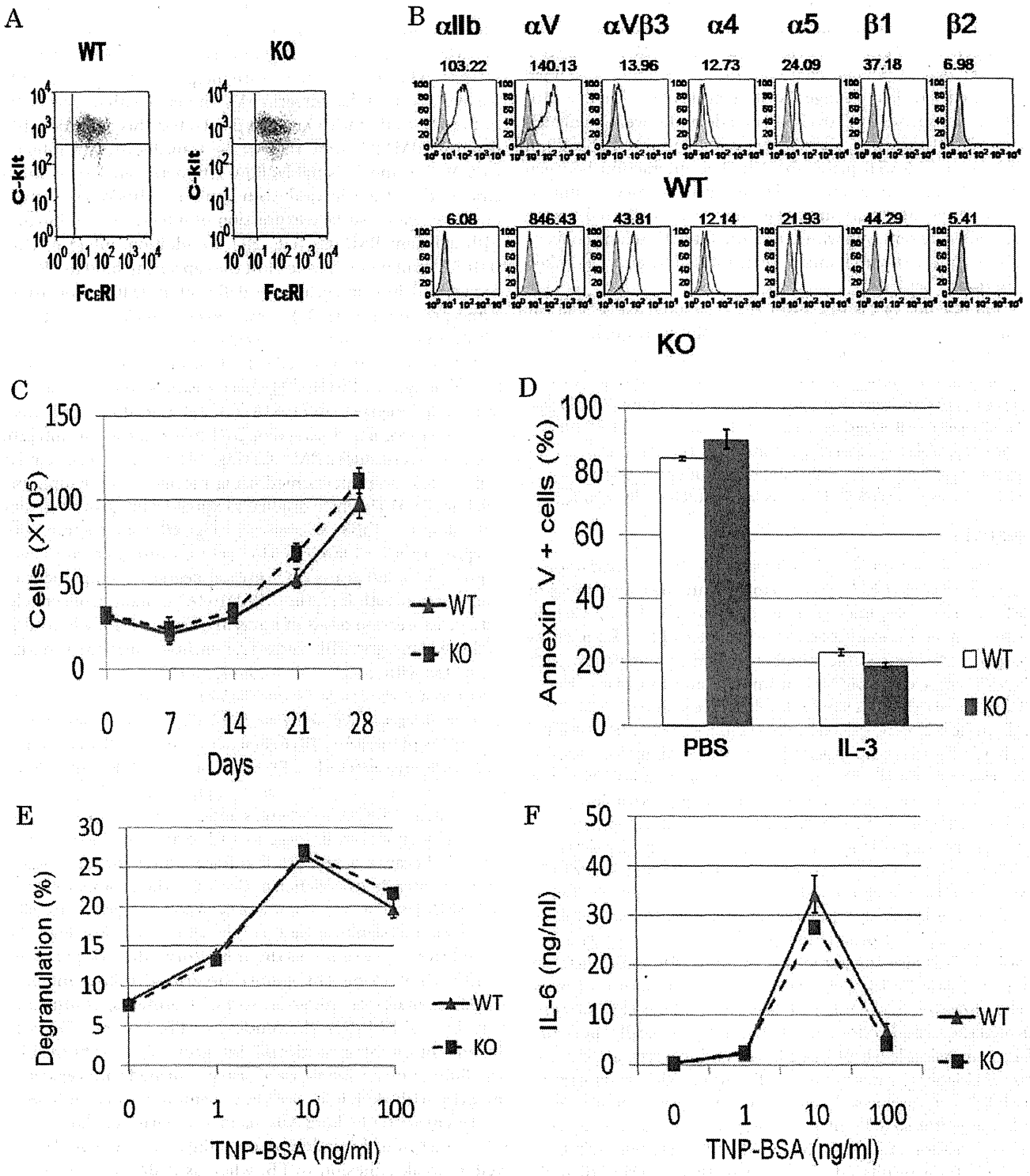

FIGURE 1. **Functional analysis of WT and integrin αIIb-deficient BMMCs in *in vitro* suspension culture.** *A* and *B*, surface expression levels of FcεRI and c-kit as well as several integrins such as integrin αIIb, αV, αVβ3, α4, α5, β1, and β2 in WT and integrin αIIb-deficient BMMCs. Mean fluorescent intensities of staining were indicated. Data are representative of three independent experiments. *C*, *in vitro* growth curves of bone marrow cells derived from WT and integrin αIIb-deficient mice. Numbers of trypan blue-excluding cells in bone marrow cell cultures in IL-3-containing medium were counted weekly. Data are representative of three independent experiments. All data points correspond to the mean ± S.D. *D*, IL-3 deprivation-induced apoptosis of WT and integrin αIIb-deficient BMMCs. Percentage of annexin V-positive cells after 48 h was measured by flow cytometric analysis. Data represent three independent experiments. All data points correspond to the mean ± S.D. *E* and *F*, after IgE-sensitized WT and integrin αIIb-deficient BMMCs were stimulated with the indicated concentrations of antigen for 50 min or 24 h, the amounts of β-hexosaminidase (*E*) or IL-6 (*F*), respectively, released into medium were measured. Data represent three independent experiments. All data points correspond to the mean ± S.D.

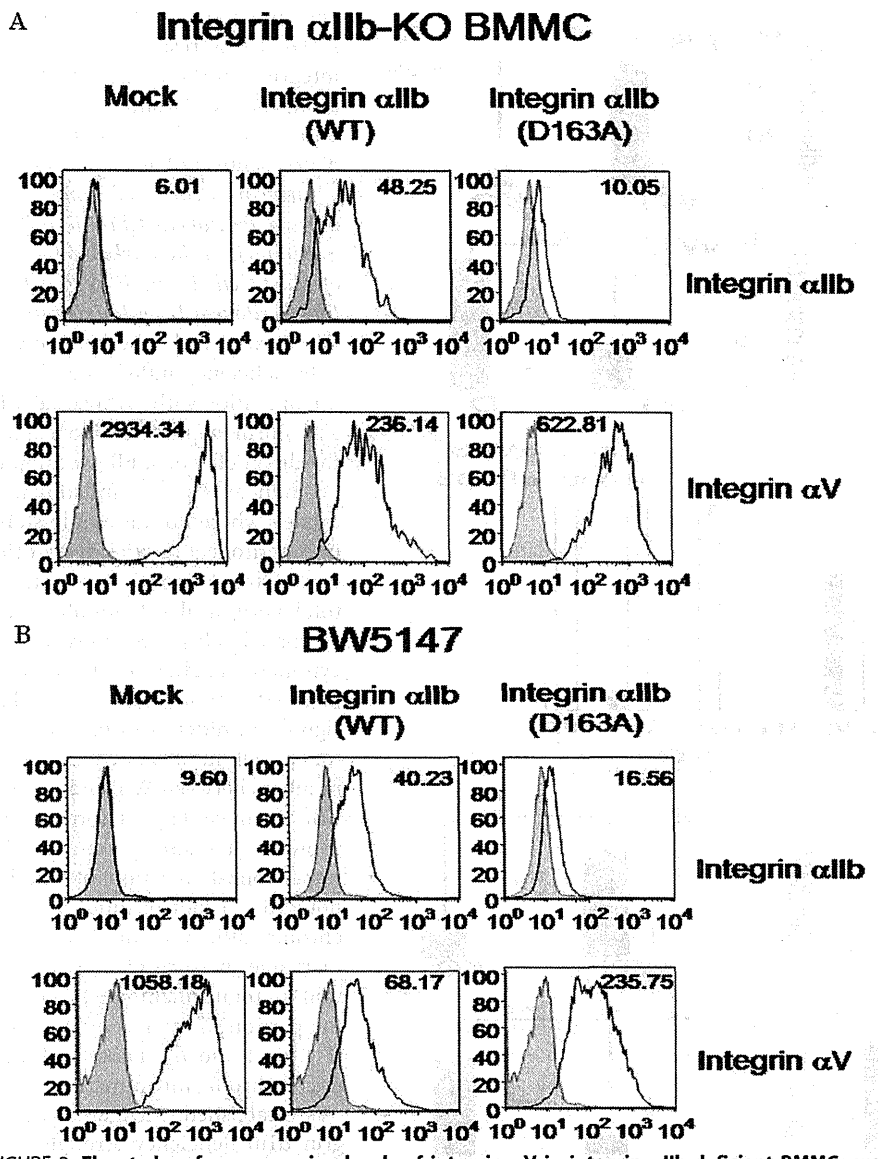

FIGURE 2. **Elevated surface expression levels of integrin αV in integrin αIIb-deficient BMMCs were reduced by transduction with integrin αIIb.** *A* and *B*, integrin αIIb-deficient BMMCs (*A*) or BW5147 cells (*B*) were transduced with integrin αIIb(WT), αIIb(D163A) mutant, or mock. Surface expression levels of integrin αIIb or integrin αV in these transfectants were analyzed by flow cytometry. Mean fluorescent intensities of staining were indicated. Data represent three independent experiments.

Enhancement of Migration, Proliferation, Degranulation, and Cytokine Production of BMMCs through Interaction with FB Is Dependent on Integrin αIIb—We next examined the effect of integrin αIIb deficiency on mast-cell functions through interaction with FB. As previously reported, SCF induced migration of WT BMMCs when the lower membranes of the Transwells were pre-coated with FB, FN, or VN. Comparison of the migrating cell numbers between WT and integrin αIIb-deficient BMMCs revealed that integrin αIIb deficiency strongly diminished or enhanced the migration of BMMCs through interaction with FB or VN, respectively, whereas it did not affect mast cell migration through interaction with FN (Fig. 3*C*). These results also suggested that, in integrin αIIb-deficient BMMCs, both the adhesive and migratory ability were altered toward integrin αVβ3, whereas there was little interaction with FB, a specific ligand for integrin αIIbβ3. Moreover, it was found in WT, but not integrin αIIb-deficient, BMMCs that SCF-stimulated mast-cell proliferation was accelerated in FB-coated plates as compared with BSA-coated plates (Fig. 4*A*). Similarly, when stimulated by IgE plus antigen, WT, but not integrin αIIb-deficient, BMMCs enhanced β-hexosaminidase release and cytokine (IL-6 and TNF-α) production through interaction with FB (Fig. 4, *B–D*). Altogether, integrin αIIbβ3 plays crucial roles in enhancing mast-cell functions through interaction with FB.

Transduction with Integrin αIIb-(WT), but Not Integrin αIIb(D163A) Mutant, into Integrin αIIb-deficient BMMCs Recovered Mast Cell Functions through Interaction with FB—To further reduce the possibility that enhanced expression levels of integrin αVβ3 modulated mast-cell functions through interaction with FB, we performed similar experiments on adhesion and cytokine production in integrin αIIb-deficient BMMCs transduced with integrin αIIb(WT), integrin αIIb-(D163A) mutant, or mock. As depicted in Fig. 5*A*, transduction with integrin αIIb(WT), but not integrin αIIb(D163A) mutant, augmented the adhesion to FB as compared with transduction with mock. On the other hand, transduction with integrin αIIb(D163A) as well as integrin αIIb(WT) diminished the adhesion to VN, with the degree of the former being a little lower than that of the latter, which was consistent with surface expression levels of integrin αVβ3 in integrin αIIb-deficient BMMCs transduced with integrin αIIb(WT) and (D163A) mutant (Fig. 2*A*). Moreover, transduction with integrin αIIb(WT), but not integrin αIIb(D163A), induced the enhancement of cytokine production through interaction with FB in integrin αIIb-deficient BMMCs (Fig. 5*B*). Collectively, these results definitively confirmed that enhanced mast cell functions through interaction with FB were dependent on integrin αIIbβ3 but not integrin αVβ3.

Integrin αIIb Deficiency Affected Neither Tissue Mast Cell Numbers in Steady States nor Mast Cell-mediated Acute Allergic Reactions—Because enhanced proliferation and migration of BMMCs through interaction with FB were suppressed by integrin αIIb deficiency, we compared the quantity of tissue mast cells in WT and in integrin $\alpha IIb^{-/-}$ mice. Microscopic

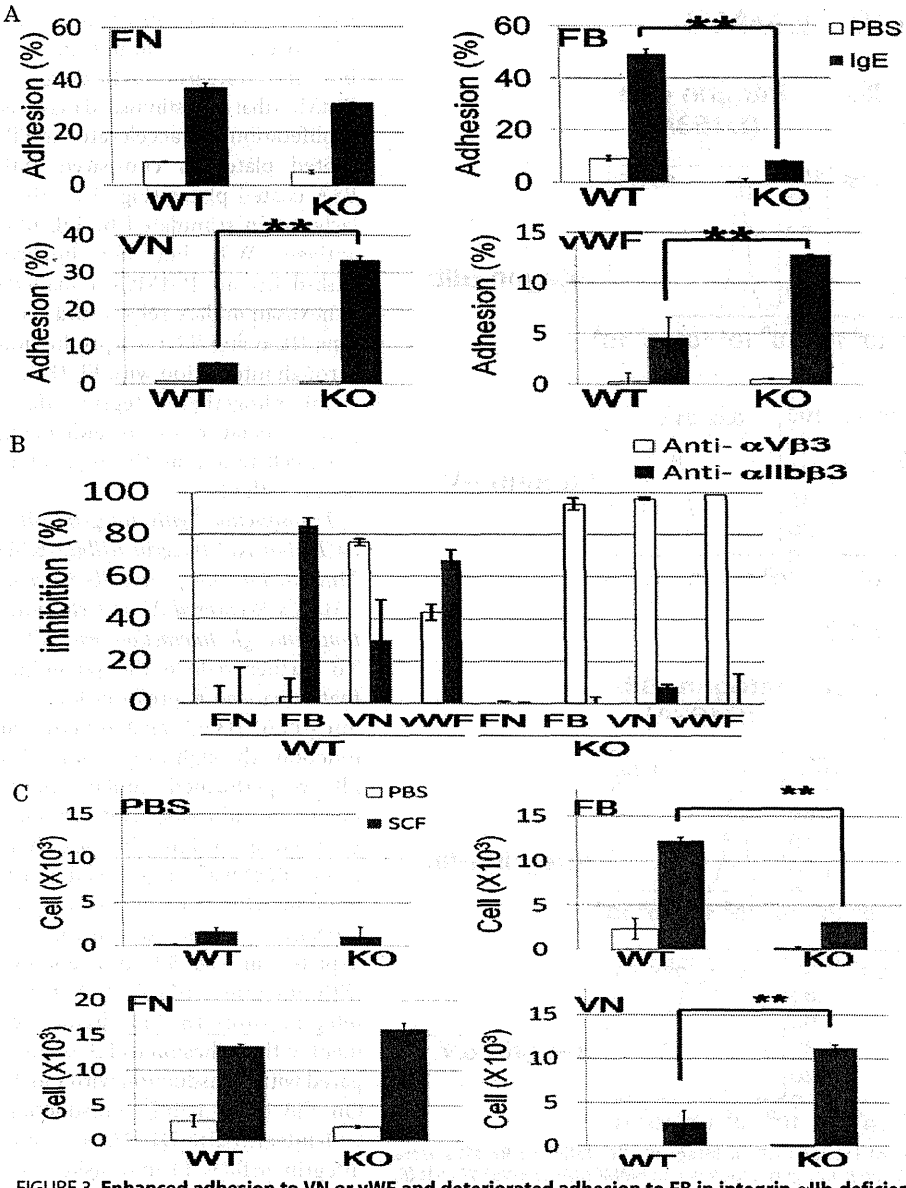

FIGURE 3. **Enhanced adhesion to VN or vWF and deteriorated adhesion to FB in integrin αIIb-deficient BMMCs.** *A*, WT and integrin αIIb-deficient BMMCs were incubated with or without 5 μg/ml SPE-7 IgE in FN-, FB-, VN-, or vWF-coated plates. Percentage of adherent cells was measured. Data are representative of three independent experiments. All data points correspond to the mean ± S.D. ** ($p < 0.01$) and * ($p < 0.05$) indicate statistical differences. *B*, pretreatment with blocking Ab for integrin αIIb or integrin αV inhibited to various degrees the adhesion of WT- or integrin αIIb-deficient BMMCs stimulated by 5 μg/ml IgE in FN-, FB-, VN-, or vWF-coated plates. Percentage of inhibition was measured. Data are representative of three independent experiments. All data points correspond to the mean ± S.D. *C*, WT or integrin αIIb-deficient BMMCs in the upper wells were attracted by 100 ng/ml SCF in the lower wells through BSA-, FB-, FN-, or VN-coated Transwells. Migrated cells were counted. Data represent three independent experiments. All data points correspond to the mean ± S.D. ** ($p < 0.01$) indicates statistical differences.

analysis demonstrated that mast-cell numbers in the ear skin, back skin, peritoneum wall, and small intestine were not different in these mice (Table 1). Based on this, we addressed the question of whether tissue FB extravasated by acute inflammation modulated mast cell-associated allergic reactions of WT and integrin $\alpha IIb^{-/-}$ mice. However, no significant difference of two types of PCA reaction was observed in these mice (data not shown), despite enhanced *in vitro* degranulation and cytokine production of mast cells through integrin αIIbβ3-dependent interaction with FB (Fig. 4, *B–D*). These results indicated that integrin αIIbβ3 was not involved in tissue mast-cell numbers and distributions in steady states or IgE-mediated acute allergic responses.

Integrin αIIb Deficiency Suppressed Peritoneal Chronic Inflammation with a Remarkable Increase of Mast Cells Induced by Repetitive Intraperitoneal FB Administration—We next asked whether integrin αIIb deficiency influenced chronic inflammation with extravascular FB and fibrin deposition. To explore the direct effects of FB, we adopted FB-induced chronic inflammation models where FB was administered into peritoneal cavities every other day. After 1 month, we counted total peritoneal cell numbers and estimated cell populations by flow cytometric analysis. In steady states before the stimulation, we found no significant differences in total peritoneal cell numbers or in mast cell numbers between WT and integrin $\alpha IIb^{-/-}$ mice (Fig. 6*A* and data not shown). Interestingly, repetitive intraperitoneal injection of FB, but not PBS as a control, induced severe chronic inflammation with a remarkable increase of mast cells as well as total inflammatory cells in the peritoneal cavities of WT mice (Fig. 6, *A* and *B*). Thus, an FB-induced chronic inflammation model was established. Intriguingly, integrin αIIb deficiency strongly suppressed the number of mast cells as well as the total number of inflammatory cells in the peritoneal cavities (Fig. 6, *A* and *B*), although the percentages of granulocytes and macrophages were not significantly different in the WT and integrin $\alpha IIb^{-/-}$ mice (Fig. 6*B*, *right panel*). Considering the *in vitro* roles of mast cell integrin αIIβ3-FB interaction, these results strongly suggested that *in vivo* FB-induced chronic inflammation was largely dependent on integrin αIIbβ3 in mast cells, although the effect of few, if any, platelets in the peritoneal cavities on this phenomenon was not completely ruled out. In addition, we found comparable numbers of inflammatory cells in WT and integrin αIIb-deficient mice 24 h after single dose of FB injection (data not shown). Therefore, FB-induced chronic inflammation required continuous administration of FB. Collectively, integrin αIIbβ3 in mast cells played

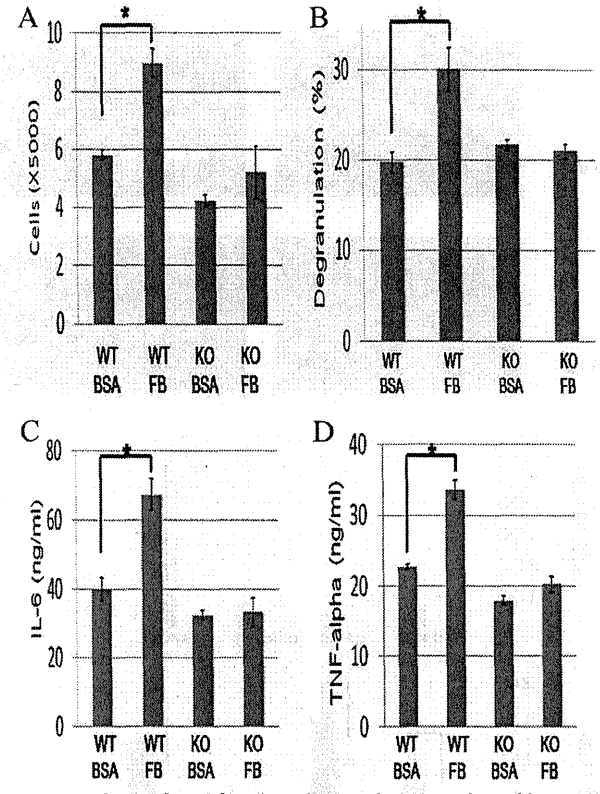

FIGURE 4. **Enhanced proliferation, degranulation, and cytokine production of WT, but not integrin αIIb-deficient, BMMCs through interaction with FB.** *A*, cell numbers of WT or integrin αIIb-deficient BMMCs stimulated by 10 ng/ml IL-3 plus 100 ng/ml SCF for 5 days in BSA- or FB-coated plates. *B*, β-hexosaminidase release of IgE-sensitized WT or integrin αIIb-deficient BMMCs stimulated by 30 ng/ml TNP-BSA for 60 min in BSA- or FB-coated plates. *C* and *D*, IL-6 (*C*) and TNF-α (*D*) production of IgE-sensitized WT or integrin αIIb-deficient BMMCs stimulated by 30 ng/ml TNP-BSA for 16 h in BSA- or FB-coated plates. All data are representative of four independent experiments. All data points correspond to the mean ± S.D. * ($p < 0.05$) indicates statistical differences.

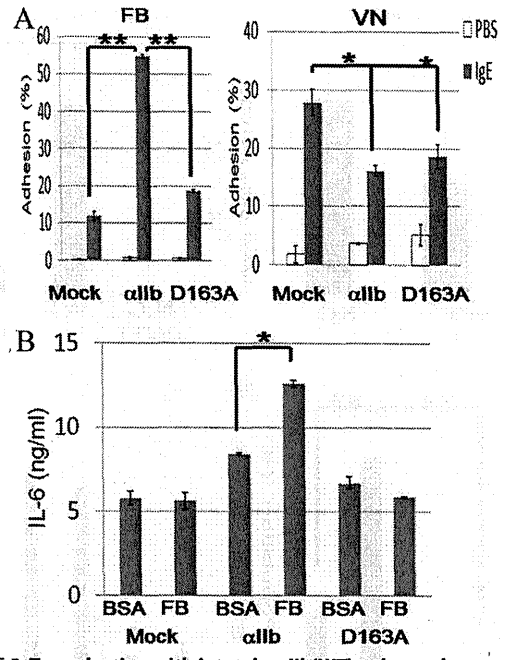

FIGURE 5. **Transduction with integrin αIIb(WT) enhanced or suppressed the adhesion to FB or VN, respectively, in integrin αIIb-deficient BMMCs.** *A*, integrin αIIb-deficient BMMCs transduced with integrin αIIb(WT), αIIb(D163A) mutant, or mock were incubated with 5 μg/ml SPE-7 IgE for 60 min in FB- or VN-coated plates. The percentage of adherent cells was measured. Data are representative of three independent experiments. All data points correspond to the mean ± S.D. ** ($p < 0.01$) and * ($p < 0.05$) indicate statistical differences. *B*, integrin αIIb-deficient BMMCs transduced with integrin αIIb(WT), αIIb(D163A) mutant, or mock were incubated with 5 μg/ml SPE-7 IgE for 16 h in FB-coated plates. The amounts of IL-6 released into medium were measured. Data are representative of three independent experiments. All data points correspond to the mean ± S.D. * ($p < 0.05$) indicates statistical differences.

TABLE 1

Numbers of mast cells in ear skin, back skin, peritoneum wall, and small intestine

Numbers of mast cells per ten randomly selected high power fields were determined under light microscopy. Results are the mean values ± S.E. for four mice/group. WT, wild type; KO, knockout.

Tissue	WT	KO
Ear skin	112 ± 11.7	109 ± 3.2
Back skin	29.7 ± 23	41.3 ± 13
Peritoneum wall	9.3 ± 5.0	10 ± 2
Small intestine	5.3 ± 3.3	6 ± 3.0

an important role in FB-mediated chronic, but not acute, inflammatory responses.

Soluble FB Enhanced Cytokine Production of WT, but Not Integrin αIIb-deficient BMMCs, in Response to S. aureus Cowan I with FB-binding Capacity—As previously reported, mast cells adhered to soluble FB as well as plate-coated FB via integrin αIIbβ3. Because soluble FB is bound by certain types of bacteria such as *S. aureus* (Cowan I), the immune cells expressing FB-binding receptors are thought to modulate the immune responses to these pathogens (23–25). We then investigated whether soluble FB influenced the response of mast cells to *S. aureus* (Cowan I). When WT or integrin αIIb-deficient BMMCs were incubated with *S. aureus* (Cowan I) for 2 h in the presence of soluble FB, fluorescent microscopic analysis demonstrated that WT, but not integrin αIIb-deficient, BMMCs were completely surrounded by aggregated *S. aureus* (Cowan I) probably through interaction with soluble FB (Fig. 7*A*). On the other hand, BMMCs were not apparently covered with *S. aureus* (Cowan I) in the absence of soluble FB. These results suggested that integrin αIIbβ3-dependent interaction of BMMCs with *S. aureus* (Cowan I) via soluble FB probably helped mast cells recognize this pathogen. Moreover, IL-6 released into each supernatant was quantified by enzyme-linked immunosorbent assay, demonstrating that soluble FB-induced enhancement of IL-6 production was observed only in WT, but not integrin αIIb-deficient, BMMCs in response to *S. aureus* (Cowan I) (Fig. 7*B*). To examine the specificity of this phenomenon, similar experiments were performed using *Escherichia coli* without FB-binding capacity. As shown in Fig. 7*B*, soluble FB-dependent enhancement of IL-6 production of BMMCs stimulated by *E. coli* was not observed irrespective of integrin αIIb expression, suggesting that soluble FB induced the enhancement of cytokine production of BMMCs in response to bacteria with, but not without, FB-binding capacity. Because Toll-like receptors primarily play an important part in the recognition of and response to bacteria (3), we also asked if soluble FB or immobilized FB enhanced cytokine production of both BMMCs stimulated by LPS, a Toll-like receptor 4 agonist. As

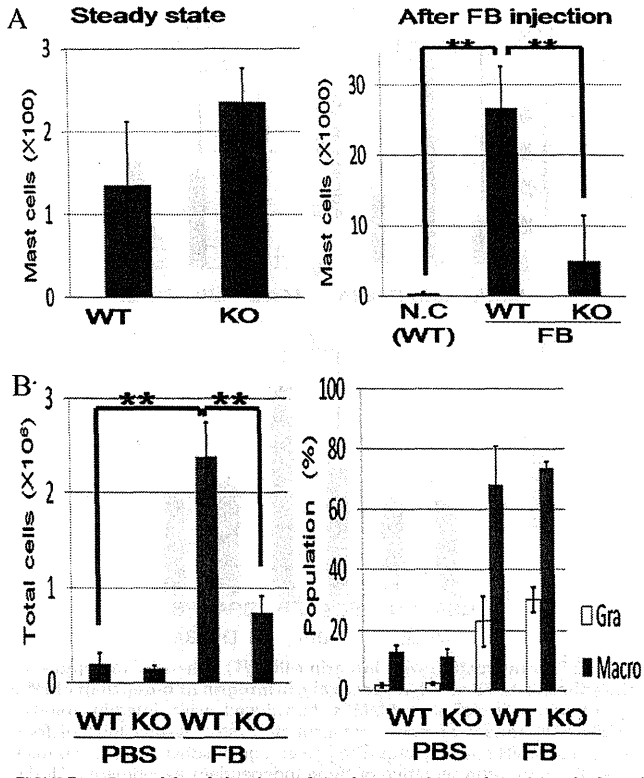

FIGURE 6. **Repetitive injection of FB into peritoneal cavities induced chronic inflammation more severely in WT mice in comparison to integrin αIIb-deficient mice.** *A*, peritoneal mast cell numbers of WT and integrin αIIb-deficient mice before (*left panel*) and after (*right panel*) FB injection. *B*, total peritoneal cell numbers (*left panel*) and cell populations (*right panel*) of WT and integrin αIIb-deficient mice after continuous intraperitoneal inoculation of FB or PBS for 1 month ($n = 5$/genotype). All data points correspond to the mean ± S.D. ** ($p < 0.01$) indicates statistical differences.

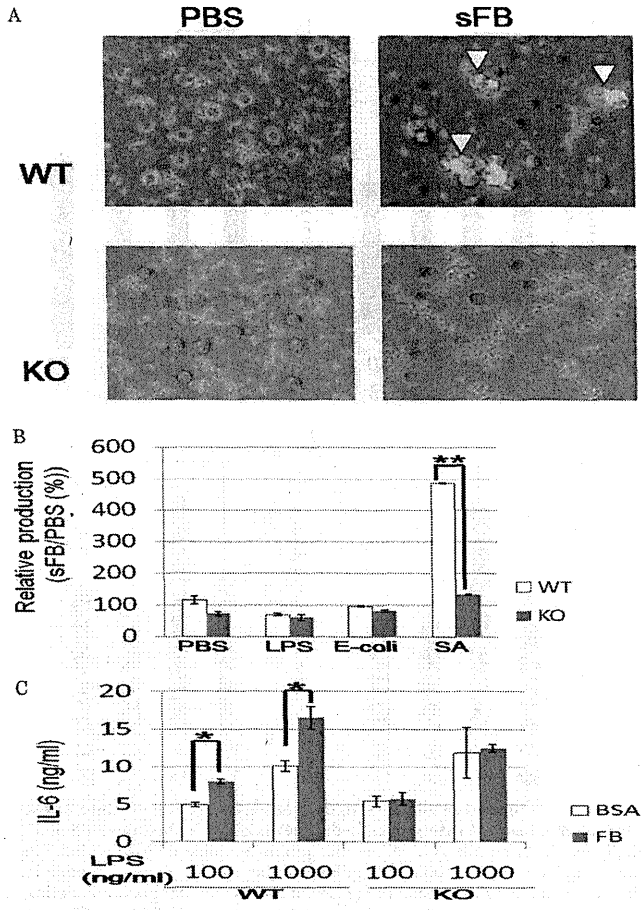

FIGURE 7. **Soluble FB enhanced cytokine production of WT, but not integrin αIIb-deficient, BMMCs in response to *S. aureus* with FB-binding capacity.** *A*, WT or integrin αIIb-deficient BMMCs were incubated with heat-killed *S. aureus* labeled by Cell Tracker Orange in the presence or absence of 500 μg/ml soluble FB for 2 h. WT, but not integrin αIIb-deficient, BMMCs were covered with SA aggregates in the presence of soluble FB (*arrowhead*). *B*, WT or integrin αIIb-deficient BMMCs were incubated with 100 ng/ml LPS, 100 μg/ml heat-killed *E. coli*, 100 μg/ml *S. aureus*, or PBS as control in the presence or absence of 500 μg/ml soluble FB for 8 h. The ratio of the amounts of IL-6 released in the presence of soluble FB to those of IL-6 in the absence of soluble FB was measured. Data are representative of three independent experiments. All data points correspond to the mean ± S.D. ** ($p < 0.01$) indicates statistical differences. *C*, WT or integrin αIIb-deficient BMMCs were incubated with the indicated concentrations of LPS in FB- or BSA-coated plates. Data represent three independent experiments. All data points correspond to the mean ± S.D. * ($p < 0.05$) indicate statistical differences.

depicted in Fig. 7 (*B* and *C*), soluble FB did not affect IL-6 production of either WT or integrin αIIb-deficient BMMCs stimulated by LPS, whereas immobilized FB enhanced IL-6 production of WT, but not integrin αIIb-deficient, BMMCs stimulated by LPS. These results suggested the synergism of Toll-like receptor 4 signaling and integrin αIIbβ3 signaling through interaction with immobilized FB, but not soluble FB. Altogether, soluble FB enhances the cytokine production of BMMCs in responses to *S. aureus* (Cowan I), probably because mast cell-soluble FB-*S. aureus* (Cowan I) complex formation promoted the quick and tight recognition of this pathogen by mast cells.

DISCUSSION

In a previous study, we found that integrin αIIbβ3 is highly expressed in mast cells, in addition to the megakaryocyte/platelet lineage and a subset of hematopoietic progenitors (9, 14, 18). Experiments using blocking Abs specific for integrins demonstrated that adhesion to FB, VN, or vWF was mediated through integrin αIIbβ3, integrin αVβ3, or both, respectively (9). In the follow-up study, we first paid attention to the interesting results shown by Berlanga O *et al.* that integrin αIIb-deficient BMMCs displayed extremely higher surface expression levels of integrin αVβ3 as compared with WT counterparts (18). Because counter-regulation of integrin αIIbβ3 and integrin αVβ3 on their surface expression levels might affect *in vivo* functions of integrin αIIbβ3 in mast cells, we attempted to delineate the underlying mechanism. Our hypothesis that integrin αIIb competed with integrin αV in heterodimerization with integrin β3 in mast cells was illustrated by experimental results as follows: retroviral transduction with integrin αIIb(WT) into integrin αIIb-deficient BMMCs reduced surface expression of integrin αVβ3 at levels comparable to those in WT BMMCs (Fig. 2*A*). In addition, transduction with integrin αIIb(D163A) mutant led to less reduction in surface expression levels of integrin αVβ3 together with less induction in those of integrin αIIbβ3 in integrin αIIb-deficient BMMCs. Thus, surface expression levels of integrin αVβ3 were conversely related to those of integrin αIIbβ3 in mast cells (Fig. 2*A*). Notably, this phenomena was true for BW5147 cells transduced with integrin αIIb(WT) or

αIIb(D163A) mutant (Fig. 2*B*). However, integrin αIIb deficiency did not affect surface expression levels of integrin αVβ3 in platelets (data not shown). These results suggested that regulatory mechanisms on surface expression levels of integrin αVβ3 differed between mast cells and platelets. One possible explanation is as follows: integrin αIIb deficiency might fail to influence surface expression levels of integrin αVβ3 if integrin β3 expression were sufficient in platelets, whereas it might promote the association of integrin αV with integrin β3 if integrin β3 expression were insufficient in mast cells. Further examination is necessary to fully understand the mechanism. Importantly, all the functional analyses (Figs. 2–4) showed that higher surface expression levels of integrin αVβ3 in integrin αIIb-deficient BMMCs enhanced adhesion to VN or vWF but did not compensate for the loss of mast-cell functions through interaction with FB. Based on this, we compared *in vivo* mast cell functions between WT and integrin αIIb-deficient mice.

First, integrin αIIb deficiency did not affect mast-cell numbers in tissues under normal conditions (Table 1). This seems reasonable, given that FB is not abundant outside blood vessels under normal conditions. Second, integrin αIIb deficiency did not affect two types of PCA estimated by ear dye extravasation or swelling (data not shown), which was reported to be mast cell-dependent (32–34). These results indicate that extravascular FB and fibrin accompanied by acute inflammation are unable to enhance mast-cell functions. On the other hand, recent advances demonstrate that FB is a central regulator of the inflammatory response as well as of hemostasis. Analysis of gene-targeted mice expressing a mutant form of FB, lacking the integrin $\alpha_M\beta2$-binding motif, demonstrated that the high affinity engagement of FB by integrin $\alpha_M\beta2$ in neutrophils and macrophages was critical for inflammatory responses (38, 39). Therefore, we speculated that FB extravasated at acute inflammatory sites activated neutrophils and macrophages via integrin $\alpha_M\beta2$ but failed to enhance mast-cell functions via integrin αIIbβ3. In contrast, we found striking differences between WT and integrin $\alpha IIb^{-/-}$ mice in FB-induced chronic inflammation: integrin αIIb deficiency strongly suppressed the increase of total inflammatory cells with mastocytosis in the peritoneal cavities. However, administration of single dose FB did not lead to any significant difference of initial inflammatory responses in these mice 24 h after inoculation (data not shown), confirming the negligible role of integrin αIIb in acute inflammation. Taking into consideration that platelets are absent in the peritoneal cavities and that integrin αVβ3 did not significantly affect *in vitro* mast-cell functions through interaction with FB, we concluded that FB-induced chronic inflammation depended on integrin αIIbβ3 in mast cells. The relevant mechanism might be as follows: FB activates macrophages and granulocytes via integrin $\alpha_M\beta2$ to produce inflammatory cytokines and chemokines in the initial phase, leading to the gradual recruitment, proliferation, and activation of mast cells in the presence of FB. Alternatively, activated mast cells also produce a diverse array of chemical mediators, accelerating chronic inflammation. Thus, FB-mediated inflammation appears to be augmented with the increase of mast cells in tissues. This scenario may explain in part why mast cell numbers increase in a variety of chronic inflammatory diseases such as atopic dermatitis and asthma that are thought to cause continuous extravasation of FB in tissues. Further analysis of WT and integrin αIIb-deficient mice using different types of chronic inflammation models will be required to delineate the role of mast cell integrin αIIbβ3 in chronic inflammatory diseases.

Another important finding in this study was that soluble FB enhanced IL-6 production of WT, but not integrin αIIb-deficient, BMMCs in response to *S. aureus* (Cowan I) with FB-binding capacity. On the other hand, soluble FB failed to enhance IL-6 production of WT BMMCs stimulated by *E. coli* harboring no FB-binding capacity, LPS, or bacterial lipopeptide (Fig. 7*B* and data not shown). Because WT, but not integrin αIIb-deficient, BMMCs apparently kept a strong contact with aggregated *S. aureus* (Cowan I) in the presence of soluble FB, integrin αIIbβ3-dependent recognition of *S. aureus* (Cowan I) in mast cells may augment the innate response to this pathogen. Considering that soluble FB facilitates the interaction of platelets with *S. aureus* by bridging clumping factor A in *S. aureus* and integrin αIIbβ3 in platelets (23–25), a similar mechanism probably occurs in mast cells: the complex formation of mast cell integrin αIIbβ3-FB-*S. aureus* (Cowan I) promotes quick and tight recognition of this pathogen by mast cells, thereby enhancing innate immune responses. Collectively, these results suggested that integrin αIIbβ3 plays an important part in the innate responses of mast cells to certain types of bacteria with FB-binding capacity.

In conclusion, the integrin αIIbβ3-dependent interaction of mast cells with FB augments FB-associated chronic inflammation or innate responses to FB-binding bacteria. Elucidation of the *in vivo* function of integrin αIIbβ3 in mast cells will lead to new approaches in the prevention of and therapy for the relevant inflammatory and infectious diseases.

Acknowledgments—We thank Drs. B. S. Coller, V. L. Woods, D. J. Gerber, and S. Tonegawa for providing Abs. We thank Dr. R. Basani for providing plasmid. We are grateful to Dr. Dovie Wylie for her excellent language assistance.

REFERENCES

1. Kawakami, T., and Galli, S. J. (2002) *Nat. Rev. Immunol.* **2,** 773–786
2. Kalesnikoff, J., and Galli, S. J. (2008) *Nat. Immunol.* **9,** 1215–1223
3. Marshall, J. S. (2004) *Nat. Rev. Immunol.* **4,** 787–799
4. Kawakami, T., and Kitaura, J. (2005) *J. Immunol.* **175,** 4167–4173
5. Kinashi, T., and Springer, T. A. (1994) *Blood* **83,** 1033–1038
6. Kitaura, J., Eto, K., Kinoshita, T., Kawakami, Y., Leitges, M., Lowell, C. A., and Kawakami, T. (2005) *J. Immunol.* **174,** 4495–4504
7. Kitaura, J., Kinoshita, T., Matsumoto, M., Chung, S., Kawakami, Y., Leitges, M., Wu, D., Lowell, C. A., and Kawakami, T. (2005) *Blood* **105,** 3222–3229
8. Bianchine, P. J., Burd, P. R., and Metcalfe, D. D. (1992) *J. Immunol.* **149,** 3665–3671
9. Oki, T., Kitaura, J., Eto, K., Lu, Y., Maeda-Yamamoto, M., Inagaki, N., Nagai, H., Yamanishi, Y., Nakajima, H., Nakajina, H., Kumagai, H., and Kitamura, T. (2006) *J. Immunol.* **176,** 52–60
10. Gurish, M. F., Tao, H., Abonia, J. P., Arya, A., Friend, D. S., Parker, C. M., and Austen, K. F. (2001) *J. Exp. Med.* **194,** 1243–1252
11. Edelson, B. T., Li, Z., Pappan, L. K., and Zutter, M. M. (2004) *Blood.* **103,** 2214–2220
12. Knight, P. A., Wright, S. H., Brown, J. K., Huang, X., Sheppard, D., and Miller, H. R. (2002) *Am. J. Pathol.* **161,** 771–779

13. Shattil, S. J., and Newman, P. J. (2004) *Blood* **104,** 1606–1615
14. Emambokus, N. R., and Frampton, J. (2003) *Immunity* **19,** 33–45
15. Eto, K., Murphy, R., Kerrigan, S. W., Bertoni, A., Stuhlmann, H., Nakano, T., Leavitt, A. D., and Shattil, S. J. (2002) *Proc. Natl. Acad. Sci. U.S.A.* **99,** 12819–12824
16. Kieffer, N., Fitzgerald, L. A., Wolf, D., Cheresh, D. A., and Phillips, D. R. (1991) *J. Cell Biol.* **113,** 451–461
17. Suehiro, K., Smith, J. W., and Plow, E. F. (1996) *J. Biol. Chem.* **271,** 10365–10371
18. Berlanga, O., Emambokus, N., and Frampton, J. (2005) *Exp. Hematol.* **33,** 403–412
19. Mosesson, M. W. (2005) *J. Thromb. Haemost.* **3,** 1894–1904
20. Tang, L., Jennings, T. A., and Eaton, J. W. (1998) *Proc. Natl. Acad. Sci. U.S.A.* **95,** 8841–8846
21. Drew, A. F., Liu, H., Davidson, J. M., Daugherty, C. C., and Degen, J. L. (2001) *Blood* **97,** 3691–3698
22. Szaba, F. M., and Smiley, S. T. (2002) *Blood* **99,** 1053–1059
23. Fitzgerald, J. R., Foster, T. J., and Cox, D. (2006) *Nat. Rev. Microbiol.* **4,** 445–457
24. Loughman, A., Fitzgerald, J. R., Brennan, M. P., Higgins, J., Downer, R., Cox, D., and Foster, T. J. (2005) *Mol. Microbiol.* **57,** 804–818
25. Fitzgerald, J. R., Loughman, A., Keane, F., Brennan, M., Knobel, M., Higgins, J., Visai, L., Speziale, P., Cox, D., and Foster, T. J. (2006) *Mol. Microbiol.* **59,** 212–230
26. Lengweiler, S., Smyth, S. S., Jirouskova, M., Scudder, L. E., Park, H., Moran, T., and Coller, B. S. (1999) *Biochem. Biophys. Res. Commun.* **262,** 167–173
27. Gerber, D. J., Pereira, P., Huang, S. Y., Pelletier, C., and Tonegawa, S. (1996) *Proc. Natl. Acad. Sci. U.S.A.* **93,** 14698–14703
28. Kitaura, J., Song, J., Tsai, M., Asai, K., Maeda-Yamamoto, M., Mocsai, A., Kawakami, Y., Liu, F. T., Lowell, C. A., Barisas, B. G., Galli, S. J., and Kawakami, T. (2003) *Proc. Natl. Acad. Sci. U.S.A.* **100,** 12911–12916
29. Morita, S., Kojima, T., and Kitamura, T. (2000) *Gene Ther.* **7,** 1063–1066
30. Kitamura, T., Koshino, Y., Shibata, F., Oki, T., Nakajima, H., Nosaka, T., and Kumagai, H. (2003) *Exp. Hematol.* **31,** 1007–1014
31. Furumoto, Y., Nunomura, S., Terada, T., Rivera, J., and Ra, C. (2004) *J. Biol. Chem.* **279,** 49177–49187
32. Hata, D., Kawakami, Y., Inagaki, N., Lantz, C. S., Kitamura, T., Khan, W. N., Maeda-Yamamoto, M., Miura, T., Han, W., Hartman, S. E., Yao, L., Nagai, H., Goldfeld, A. E., Alt, F. W., Galli, S. J., Witte, O. N., and Kawakami, T. (1998) *J. Exp. Med.* **187,** 1235–1247
33. Inagaki, N., Goto, S., Nagai, H., and Koda, A. (1986) *Int. Arch. Allergy Appl. Immunol.* **81,** 58–62
34. Nagai, H., Sakurai, T., Inagaki, N., and Mori, H. (1995) *Biol. Pharm. Bull.* **18,** 239–245
35. Wong, M. X., Roberts, D., Bartley, P. A., and Jackson, D. E. (2002) *J. Immunol.* **168,** 6455–6462
36. Artis, D., Humphreys, N. E., Potten, C. S., Wagner, N., Müller, W., McDermott, J. R., Grencis, R. K., and Else, K. J. (2000) *Eur. J. Immunol.* **30,** 1656–1664
37. Honda, S., Tomiyama, Y., Shiraga, M., Tadokoro, S., Takamatsu, J., Saito, H., Kurata, Y., and Matsuzawa, Y. (1998) *J. Clin. Invest.* **102,** 1183–1192
38. Flick, M. J., LaJeunesse, C. M., Talmage, K. E., Witte, D. P., Palumbo, J. S., Pinkerton, M. D., Thornton, S., and Degen, J. L. (2007) *J. Clin. Invest.* **117,** 3224–3235
39. Flick, M. J., Du, X., Witte, D. P., Jirousková, M., Soloviev, D. A., Busuttil, S. J., Plow, E. F., and Degen, J. L. (2004) *J. Clin. Invest.* **113,** 1596–1606

Leukemia (2009) 23, 2197–2209

www.nature.com/leu

LEADING ARTICLE

Mixed-lineage-leukemia (*MLL*) fusion protein collaborates with Ras to induce acute leukemia through aberrant *Hox* expression and Raf activation

R Ono[1,2,3], H Kumagai[1], H Nakajima[4,5], A Hishiya[1,2], T Taki[6], K Horikawa[7], K Takatsu[7,8], T Satoh[9], Y Hayashi[10], T Kitamura[2] and T Nosaka[1,2,3]

[1]*Division of Hematopoietic Factors, The Institute of Medical Science, The University of Tokyo, Tokyo, Japan;* [2]*Division of Cellular Therapy, The Institute of Medical Science, The University of Tokyo, Tokyo, Japan;* [3]*Department of Microbiology and Molecular Genetics, Mie University Graduate School of Medicine, Mie, Japan;* [4]*Center of Excellence, The Institute of Medical Science, The University of Tokyo, Tokyo, Japan;* [5]*Division of Hematology, Department of Internal Medicine, Keio University School of Medicine, Tokyo, Japan;* [6]*Department of Molecular Laboratory Medicine, Kyoto Prefectural University of Medicine Graduate School of Medical Science, Kamigyo-ku, Kyoto, Japan;* [7]*Department of Immunology, The Institute of Medical Science, The University of Tokyo, Tokyo, Japan;* [8]*Department of Immunobiology and Pharmaceutical Genetics, Graduate School of Medicine and Pharmaceutical Sciences, University of Toyama, Toyama, Japan;* [9]*Division of Molecular Biology, Department of Biochemistry and Molecular Biology, Kobe University Graduate School of Medicine, Kobe, Japan and* [10]*Gunma Children's Medical Center, Gunma, Japan*

Mixed-lineage-leukemia* (*MLL*) fusion oncogenes are closely involved in infant acute leukemia, which is frequently accompanied by mutations or overexpression of *FMS-like receptor tyrosine kinase 3* (*FLT3*). Earlier studies have shown that *MLL* fusion proteins induced acute leukemia together with another mutation, such as an *FLT3* mutant, in mouse models. However, little has hitherto been elucidated regarding the molecular mechanism of the cooperativity in leukemogenesis. Using murine model systems of the *MLL*-fusion-mediated leukemogenesis leading to oncogenic transformation *in vitro* and acute leukemia *in vivo*, this study characterized the molecular network in the cooperative leukemogenesis. This research revealed that *MLL* fusion proteins cooperated with activation of Ras *in vivo*, which was substitutable for Raf *in vitro*, synergistically, but not with activation of signal transducer and activator of transcription 5 (STAT5), to induce acute leukemia *in vivo* as well as oncogenic transformation *in vitro*. Furthermore, *Hoxa9*, one of the *MLL*-targeted critical molecules, and activation of Ras *in vivo*, which was replaceable with Raf *in vitro*, were identified as fundamental components sufficient for mimicking *MLL*-fusion-mediated leukemogenesis. These findings suggest that the molecular crosstalk between aberrant expression of *Hox* molecule(s) and activated Raf may have a key role in the *MLL*-fusion-mediated-leukemogenesis, and may thus help develop the novel molecularly targeted therapy against *MLL*-related leukemia.

Leukemia (2009) **23,** 2197–2209; doi:10.1038/leu.2009.177; published online 27,August 2009
Keywords: MLL; Ras; MAP kinase; leukemogenesis

Introduction

Multistep oncogenesis has been suggested in malignancy by the observation of more than two heterogeneous genetic and/or epigenetic lesions.[1] In leukemogenesis, recurring chromosomal translocations are frequently found in hematological malignancies, which sometimes coincide with subtle but critical genetic mutations leading to functional aberration.[2–4] Earlier studies showed that many of the translocation target genes are transcription factors involved in hematopoietic differentiation and/or self-renewal, whereas coincident mutations often occur on the genes involved in cell proliferation.[4] These results lead to a hypothetical model of leukemogenesis in which these two kinds of genetic alterations may cooperate to induce acute leukemia. This concept has been recently exemplified in experimental models using combinations of fusion genes, including *mixed-lineage leukemia* (*MLL*, also called *ALL1* or *HRX*) or *AML1* fusion genes, and other coincident genetic mutations.[5–9]

MLL is a proto-oncogene that is rearranged in human acute leukemia with chromosome 11 band q23 (11q23) translocation,[10,11] encoding a histone methyltransferase that assembles in a chromatin-modifying supercomplex.[12] Meanwhile, *MLL* fusion gene leads to leukemogenesis through several *HOX* genes directly transactivated by *MLL* fusion protein itself.[4,11,13,14] It is noteworthy that most of the genetically engineered mice carrying the *MLL* fusion developed hematological malignancy after a long latency, suggesting that secondary genotoxic stress is required to develop overt acute leukemia.[15–18] An earlier study presented direct evidence that *MLL* fusion proteins induced myeloproliferative disease (MPD) with a long latency, and caused acute leukemia with a short latency together with a coincident mutation of *FMS-like tyrosine kinase 3* (*FLT3*).[6]

Recent studies revealed that genetic alterations, including *FLT3*, *NRAS* (neuroblastoma RAS viral (v-ras) oncogene homolog) and *KRAS* (v-Ki-ras2 Kirsten rat sarcoma viral oncogene homolog), are frequently accompanied by 11q23 translocation.[19,20] *FLT3* is a receptor tyrosine kinase involved in leukemogenesis and normal hematopoiesis.[21] The mutations of *FLT3* are mainly classified into length mutations such as internal tandem duplication (ITD) of the juxtamembrane domain, and point mutations within the activation loop of the second tyrosine kinase domain (TKD).[21] Interestingly, *FLT3*-TKD, as well as overexpression of the wild type of FLT3, is found to be frequently associated with infant acute lymphoid leukemia (ALL), with rearrangements of *MLL*.[19,22] Both types of *FLT3* mutations result in a constitutive activation of *FLT3* kinase activity, followed by activation of signaling pathways, including signal transducer and activator of transcription 5 (STAT5) and Ras/Raf/mitogen-activated protein (MAP) kinase.[23,24] Both STAT5 and Ras/Raf/MAP kinase (MAPK) are involved in cellular

Correspondence: Dr T Nosaka, Department of Microbiology and Molecular Genetics, Mie University Graduate School of Medicine, 2-174 Edobashi, Tsu, Mie 514-8507, Japan.
E-mail: nosaka@doc.medic.mie-u.ac.jp
Received 1 October 2008; revised 17 July 2009; accepted 21 July 2009; published online 27 August 2009

proliferation, survival and differentiation.[25,26] Constitutively active mutants of Ras induce oncogenic transformation through activation of the MAPK cascade.[26] However, little has so far been elucidated regarding the molecular mechanism of collaboration in leukemogenesis.

To further clarify the molecular mechanism of *MLL*-fusion-mediated leukemogenesis, we focused on signal transduction associated with malignant transformation that collaborates with *MLL* fusion protein *in vitro*, and highlighted the contrastive roles of STAT5 and MAPK in leukemogenesis. Interestingly, comparative analyses suggested synergistic collaboration with activated Ras in *MLL*-fusion-mediated leukemogenesis, and also activation of Raf in malignant transformation *in vitro*, but not with STAT5 activation *in vivo* and *in vitro*. Thus, the activation of Ras/Raf/MAPK cascade may have an important role in multistep leukemogenesis with 11q23 translocations.

Materials and methods

Construction of the plasmids and retrovirus production

Fragments of murine constitutively active mutants of STAT5A (#2[27] and 1*6[28]) fused with a FLAG tag at the C-terminus, a coding region of human *NRAS*^{G12V} and *MLL-eleven nineteen leukemia* (*ENL*) short form[6] were inserted upstream of the internal ribosomal entry site (IRES)-enhanced green fluorescent protein (EGFP) cassette of pMYs-IRES-EGFP.[29] Fragments of coding regions of a wild type of *NRAS* and *NRAS*^{G12V} were inserted into pMXs-puro.[29] A fragment of murine *Hoxa9*[30] (a kind gift from Dr G Sauvageau) was inserted into pMXs-IRES-EGFP.[29] A fragment of a dominant negative mutant (dn) of STAT5A[23] was inserted upstream of the IRES-Kusabira-Orange (KO)[31] cassette of pMXs-IRES-KO, in which the EGFP cassette in pMXs-IRES-EGFP[29] was replaced with the KO cassette of phKO1-S1 (MBL, Nagoya, Japan). pMXs-neo-*MLL-SEPT6*,[6] pMY-FLT3-ITD-IRES-EGFP,[6] pMY-FLT3^{D835V}-IRES-EGFP[6] and pBabe-puro-Δ*Raf*-estrogen receptor (ER)[28] were described earlier. Retroviruses were harvested 48 h after transfection with each retroviral construct into PlatE cells[29] in which appropriate expression of the transgenes was confirmed by western blot analysis, as described earlier.[6]

Cells

An *MLL-SEPT6*-immortalized murine myelomonocytic cell line, HF6, was established through colony-replating assays using retroviral transduction with pMXs-neo-*MLL-SEPT6* as described earlier.[6] A *Hoxa9*-immortalized murine myelomonocytic cell line, A9G, was established through infection with retroviruses harboring *Hoxa9* in pMXs/IRES-EGFP[29] as reported earlier.[32] The HF6,[6] A9G and murine pro-B Ba/F3[28] cells were cultured in the presence of interleukin-3 (IL-3) (R&D Systems, Minneapolis, MN, USA). HF6 cells transduced with *FLT3* mutants were cultured in the same medium, except for the absence of IL-3. The expression levels of *FLT3* in these cells were evaluated using a phycoerythrin (PE)-conjugated anti-CD135 antibody, or an anti-mouse immunoglobulin G1,κ, as the isotype-matched control (BD Biosciences, San Diego, CA, USA) using fluorescence-activated cell sorting (FACS) Calibur (BD Biosciences) as described earlier.[33]

Immunoprecipitation and western blot analysis

Fifty million parental and additionally transduced HF6 cells, or 10 million parental and transduced Ba/F3 cells, were harvested in the lysis buffer, and the lysates were either suspended with 1 × sodium dodecyl sulfate sample buffer after immunoprecipitation using polyclonal anti-STAT5A antibody (L-20) (Santa Cruz Biotechnology, Santa Cruz, CA, USA) or directly mixed with an equal volume of 2 × sodium dodecyl sulfate sample buffer and then boiled, as described earlier.[25] In some experiments, the parental HF6 cells had been deprived of IL-3 8 h before harvest. Western blot analysis of each sample was performed using the polyclonal anti-STAT5A (L-20), monoclonal anti-phosphotyrosine (4G10) (Upstate Biotechnology, Lake Placid, NY, USA), polyclonal anti-extracellular signal-related kinase (ERK)1/2, monoclonal anti-phospho-ERK1/2 (E10) (Cell Signaling Technology, Danvers, MA, USA), monoclonal anti-α-tubulin (Sigma-Aldrich, St Louis, MO, USA), monoclonal anti-FLAG (M2), polyclonal anti-ERα (MC-20) and monoclonal anti-N-Ras (F155) (Santa Cruz Biotechnology) antibodies to probe membranes, as described earlier.[25]

Evaluation of cellular effects by inhibition of signal transduction in vitro

The response to the drug was evaluated as described earlier.[23] In brief, HF6 cells expressing the *FLT3* mutants (3×10^5) were infected with retroviruses harboring or not harboring the dnSTAT5A in pMXs-IRES-KO in the presence of polybrene, as described earlier.[6] Viable cell numbers were counted with standard Trypan blue staining, and the expression of the dnSTAT5A was monitored by assessment of KO positivity using the FL2 channel on the FACS Calibur, daily after infection. At 48 h after infection, to evaluate the status of phosphorylated STAT5, half a million of these cells were fixed with fixation buffer, permeablized with Perm Buffer III and analyzed with an Alexa Fluor 647-conjugated anti-phospho-STAT5 (Y694) (all from BD Biosciences) antibody, or the anti-mouse immunoglobulin G1,κ, as the isotype-matched control antibody, using the FL4 channel on the FACS Calibur, according to the manufacturer's recommendation. As controls, the parental HF6 cells with and without IL-3 stimulation after deprivation of IL-3 for 8 h were used. Meanwhile, these HF6 cells (1×10^4) were cultured for 72 h in 24-well plates in the presence of various concentrations of a MAPK kinase (MEK) inhibitor, U0126, or a PI3 kinase inhibitor, LY294002 (Calbiochem-Novabiochem, San Diego, CA, USA) and each vehicle control (ethanol for U0126 and dimethyl sulfoxide for LY294002). Viable cell numbers were counted with standard Trypan blue staining after each treatment, followed by calculation of the 50% inhibitory concentration (IC50) of each drug using a logistic regression model. To evaluate the inhibitory effect of U0126 on ERK1/2, five million of the cells were treated for 2 h, harvested and analyzed with the anti-ERK1/2 or the anti phospho-ERK1/2 antibody after western blotting.

Myeloid transformation assays in vitro

In a series of transformation assays, the acquisition of IL-3-independent proliferation was examined in IL-3-dependent cells. HF6 and Ba/F3 cells were infected with retroviruses harboring *NRAS*, *NRAS*^{G12V} or mock in pMXs-puro; Δ*Raf*-ER or mock in pBabe puro; and STAT5A1*6, STAT5A#2 or none (only GFP) in pMYs-IRES-EGFP, respectively, in the presence of polybrene, as described earlier.[6] A9G cells were also retrovirally transduced with *NRAS*, *NRAS*^{G12V} Δ*Raf*-ER or each mock in the same way. For puromycin selection, the transduced cells were cultured with 1 μg/ml of puromycin 24–96 h after infection, followed by propagation for 5 days in the absence of puromycin.

Next, 1×10^5 puromycin-resistant cells transduced with *NRAS*, *NRAS*^{G12V} or mock were cultured in 24-well plates in the absence of IL-3, whereas those transduced with Δ*Raf*-ER or mock were cultured under the same condition, except for the presence of 1 μM of 4-hydroxy-tamoxifen or a vehicle control (ethanol). The cells transduced with STAT5A1*6, STAT5#2 or none were purified on the basis of the expression of GFP using a FACS Aria (BD Biosciences) 36 h after infection. Immediately, these purified cells (1×10^4) were cultured in 96-well plates in the absence of IL-3, to avoid excessive signals caused by STAT5A#2 or 1*6 in the presence of IL-3, which led to cell death as described earlier.[25] Viable cell numbers were counted periodically after standard Trypan blue staining.

Leukemogenesis assays in vivo

Leukemogenesis assays *in vivo* using C57BL/6 mice produced by a combination of two kinds of transgenes were performed with lethal conditioning using lethally (9.5 Gy) irradiated recipients, or with sublethal conditioning using sublethally (5.25 Gy) irradiated recipients receiving no radioprotective bone marrow (BM) cells, as described earlier[6] (Supplementary Figure 1). In brief, hematopoietic progenitors were harvested from 6- to 10-week-old Ly-5.1 C57BL/6 mice 4 days after intraperitoneal administration of 150 mg/kg 5-fluorouracil, and cultured overnight in alpha minimal essential medium supplemented with 20% fetal calf serum and 50 ng/ml each of mouse stem cell factor, human IL-6, human FLT3-ligand (R&D Systems) and human thrombopoietin (Kirin Brewery, Takasaki, Japan). The prestimulated cells were infected with several combinations of the retroviruses for 60 h in the α minimal essential medium supplemented with the same fetal calf serum and cytokines using RetroNectin (Takara Bio Inc., Otsu, Japan) according to the manufacturer's recommendations, followed by intravenous injection of 10^5 of the cells into Ly-5.2 mice together with either a radioprotective dose (2×10^5) of Ly-5.2 cells under lethal conditioning or none under sublethal conditioning. Morbid mice and their tissue samples were analyzed, and immunophenotyping of BM, splenic and thymic cells was performed using the FACS Calibur, as described earlier.[33] The hematopoietic neoplasms were diagnosed mainly on the basis of morphology as described earlier.[6] The probabilities of murine overall survival were estimated using Kaplan–Meier method and compared using the log-rank test. All animal studies were performed in accordance with the guidelines of the Animal Care Committees of the Institute of Medical Science, the University of Tokyo and the Mie University.

Southern blot analysis

Genomic DNA was extracted from spleens, digested with *Nhe*I or *Bam*HI for detecting proviral integration and clonality, respectively, and analyzed with the Neo or puro probe (Supplementary Figure 1) as described earlier.[34]

Reverse transcriptase-polymerase chain reaction (PCR)

Total RNA was extracted from cell lines, spleen or BM, and reverse transcribed to complementary DNA as described earlier.[6] The conditions, reagents for reverse transcriptase-PCR and the primers specific for *β*$_2$*microglobulin* (*β*$_2$*MG*), *Hoxa9* and *MLL-SEPT6* have been described earlier,[6] except that PCR amplification for *MLL-SEPT6* transcripts was sometimes run for 35 cycles. To detect the transcript of *NRAS*^{G12V}, PCR amplification was run for 21 cycles using the following primers: *NRAS-S*, 5′-GTGGTTATAGATGGTGAAACCTGTT-3′ and *NRAS-AS*, 5′-GACCATAGGTACATCTTCAGAGTCCT-3′.

Results

MLL-SEPT6 *cooperates with both types of* FLT3 *mutations through different modes of signal transduction*

To clarify the molecular mechanism of cooperation between *MLL* fusion proteins and *FLT3* mutants, signaling pathways of *FLT3*-ITD and *FLT3*-TKD that cooperate with *MLL-SEPT6* were examined using the IL-3-dependent *MLL-SEPT6*-immortalized cell line, HF6.[6] Earlier, STAT5 and MAPK ERK1/2 had been found to be activated downstream of *FLT3* mutants in factor-dependent cell lines.[23,24] Therefore, the activation of these molecules was first examined using parental HF6 and transformed HF6 cells expressing FLT3-*ITD* (HF6^{ITD}) or *FLT3*^{D835V} (HF6^{D835V}) described earlier.[6] Nearly equal levels of expression of the *FLT3* mutants in the transformed HF6 cells were confirmed (Figure 1a). A western blot analysis after immunoprecipitation of the lysates from these cells revealed constitutive phosphorylation of STAT5A in HF6 cells expressing the FLT3 mutants in the absence of IL-3, but little in the parental HF6 cells that had been deprived of IL-3 (Figure 1b). In addition, a western blot analysis of the same lysates also revealed constitutive phosphorylation of ERK1/2 in those cells expressing the *FLT3* mutants, but little in the parental HF6 cells that had been deprived of IL-3 (Figure 1b).

Next, to determine whether STAT5 and/or MAPK were important in the transformation of HF6 cells expressing *FLT3* mutants, each signaling pathway was inhibited using dnSTAT5A or MEK inhibitor U0126. After retroviral transduction with the dnSTAT5A, the proliferation of HF6^{ITD} cells expressing dnSTAT5A was suppressed more efficiently than that of HF6^{D835V} cells expressing dnSTAT5A (Figure 2a). KO-positive cells expressing dnSTAT5A showed higher levels of phosphorylated STAT5 than KO-negative cells (Figure 2b). This finding is consistent with the earlier report showing that the dnSTAT5A exerts its effect on endogenous STAT5A and 5B with persistent phosphorylation of the dnSTAT5A itself.[35] In contrast, U0126 retarded the proliferation of the HF6^{D835V} cells more effectively than the HF6^{ITD} cells (Figure 2c, each IC50 is 0.67 ± 0.35 μM for HF6^{D835V} and 6.09 ± 0.90 μM for HF6^{ITD} in the absence of IL-3). Indeed, U0126 inhibited phosphorylation of ERK1/2 in the HF6^{ITD} and HF6^{D835V} cells in a semidose-dependent manner (Figure 2d). In addition, another important signaling pathway downstream of *FLT3*, through PI3 kinase, was inhibited using LY294002. LY294002 also retarded the growth of the HF6^{D835V} and HF6^{ITD} cells in a dose-dependent manner, but there was no remarkable difference between both types of HF6 cells (Supplementary Figure 2, each IC50 is 4.18 ± 0.55 μM for HF6^{D835V} and 8.12 ± 1.54 μM for HF6^{ITD} in the absence of IL-3).

Taken together, these results *in vitro* suggested that the activation of MAPK was more critical for transformation by *FLT3*-TKD than by *FLT3*-ITD in HF6 cells, whereas activation of STAT5 was more critical for transformation by *FLT3*-ITD than by *FLT3*-TKD.

Activation of Ras-MAPK cascade enables HF6 cells to grow without IL-3 through cooperation between Hoxa9 *and Raf*

We further examined whether direct activation of either STAT5 or MAPK cascade is sufficient to confer factor-independent

growth on HF6 cells. Although the constitutively active mutants of STAT5A, the relatively stronger mutant STAT5A1*6 and weaker mutant STAT5A#2, enabled Ba/F3 cells (Ba/F3^{1*6}, Ba/F3$^{\#}$) to grow without IL-3 as reported earlier,[25,27,28] both failed to confer factor-independent growth on HF6 cells with limited elongation of survival time without IL-3 (Figures 3a and c). In contrast, the oncogenic *NRAS* mutant, *NRAS*^{G12V}, which had been detected in a case of *AML* with *MLL-SEPT6*,[20] enabled HF6 cells (HF6^{G12V}) to grow without IL-3, while it conferred no factor-independent growth on Ba/F3 with limited elongation of survival time without IL-3 (Figures 3b and c). In addition, Raf-1, a signal molecule downstream of Ras in Ras-MAPK cascades associated with malignant transformation, was tested with an activation-inducible system using Δ*Raf*-ER, consisting of the catalytic domain of human RAF-1 (ΔRaf) and the hormone-binding domain of the ER (Figure 3d), as described earlier.[28] Unlike transduced Ba/F3 (Ba/F3$^{\Delta Raf\text{-}ER}$) cells, transduced HF6 (HF6$^{\Delta Raf\text{-}ER}$) cells grew without IL-3 only in the presence of 4-hydroxy-tamoxifen (Figure 3e). In these HF6$^{\Delta Raf-ER}$ cells treated with 4-hydroxy-tamoxifen, STAT5A was not found to be secondarily activated by induction of activation of Raf/MAPK cascade in the absence of IL-3, whereas it was found to be weakly activated by stimulation with IL-3 for 15 min (data not shown).

Furthermore, we examined whether *Hoxa9*, which is one of the well-known target genes of *MLL* fusion proteins,[10,11,13,14] is involved in cooperation between *MLL* fusion protein and Ras/Raf/MAPK cascade. In the myeloid transformation assays, the murine BM progenitors immortalized by *Hoxa9* in the presence of IL-3 (named A9G) proliferated without IL-3 after retroviral transduction of *NRAS*^{G12V} (Figure 3b). In the inducible transformation system using Δ*Raf*-ER, transduced A9G

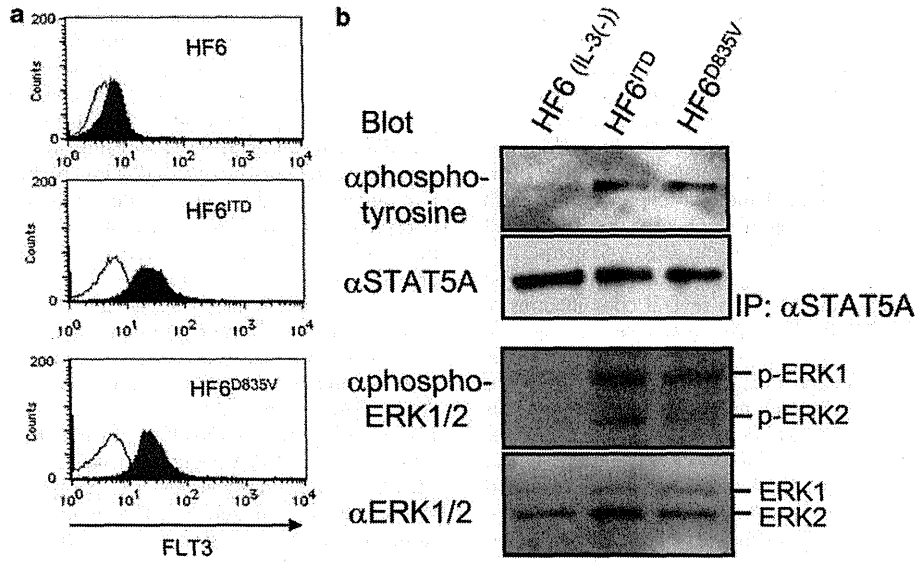

Figure 1 Characterization of signal transduction in the HF6 cells transformed by *FMS-like receptor tyrosine kinase 3* (*FLT3*) mutants. (**a**) Expression of each *FLT3* mutant in HF6 and their transformed cells. The shadow profiles and black lines represent fluorescence-activated cell sorting (FACS) staining obtained using the antibody specific to *FLT3* and its isotype control antibody, respectively. (**b**) Western blot analyses of proteins extracted from HF6 and their transformed cells after immunoprecipitation using the anti-signal transducer and activator of transcription 5A (STAT5A) antibody (upper two panels), and of the whole lysates (lower two panels). The parental HF6 cells had been deprived of interleukin-3 (IL-3) 8 h before harvest. The blot of the immunoprecipitated samples was probed with the anti-STAT5A antibody (upper bottom panel), followed by reprobe with 4G10 (the anti-phosphotyrosine antibody) (upper top panel). The blot of the whole lysates was probed with the anti-extracellular signal-related kinase (ERK)1/2 antibody (lower bottom panel), followed by reprobe with the anti-phospho-ERK1/2 antibody (lower top panel).

Figure 2 Differential effects of inhibition of cellular signal transduction on the HF6 cells transformed by *FMS-like receptor tyrosine kinase 3* (*FLT3*) mutants. (**a**) Effect of the retroviral transduction with the dominant negative mutant of signal transducer and activator of transcription 5A (dnSTAT5A) in pMXs-internal ribosomal entry site (IRES)-Kusabira-Orange (KO) on the transformed and parental HF6 cells. Viable cell numbers and KO expression were monitored daily after the transduction, and the averages of ratios of each KO-positive cell number at days 1, 2, 3 and 4 to that at day 1 are shown with s.d. (bars). (**b**) Intracellular flow cytometric analyses of phospho-STAT5 (Y694) on the transformed and parental HF6 cells transduced with dnSTAT5A in pMXs-IRES-KO. The density plots show expression of each intracellular antigen labeled with the Alexa Fluor 647-conjugated anti-phospho-STAT5 (Y694) (upper eight panels) or its isotype control (lower two panels) antibody versus expression of KO. As negative controls, nontransduced and mock-transduced HF6 cells were used, respectively (lower two panels using the isotype control antibody). As references, nontransduced HF6 cells were deprived of interleukin-3 (IL-3) for 8 h (HF6 (IL-3(−))), or stimulated with IL-3 for 15 min after the same deprivation (HF6 (IL-3(+))), and then used (lower two panels using the anti-phospho-STAT5 antibody). KO and Alexa Fluor 647 were detected using the FL2 and FL4 channels of the fluorescence-activated cell sorting (FACS) Calibur, respectively. (**c**) Effect of the various concentrations of mitogen-activated protein kinase (MAPK) kinase (MEK) inhibitor, U0126, on the transformed and the parental HF6 cells. The averages with s.d. (bars) of ratios of viable cell numbers in the presence of each concentration of U0126 to those in the absence of U0126 are shown. (**d**) Western blot analyses of the whole lysates extracted from the transformed HF6 cells treated with U0126. Both groups of transformed HF6 cells were treated with various concentrations (shown above each upper panel) of U0126 for 2 h and then harvested. Both blots were probed with the anti-phospho-extracellular signal-related kinase (ERK)1/2 antibody (each top panel), followed by reprobe with the anti-ERK1/2 antibody (each bottom panel).

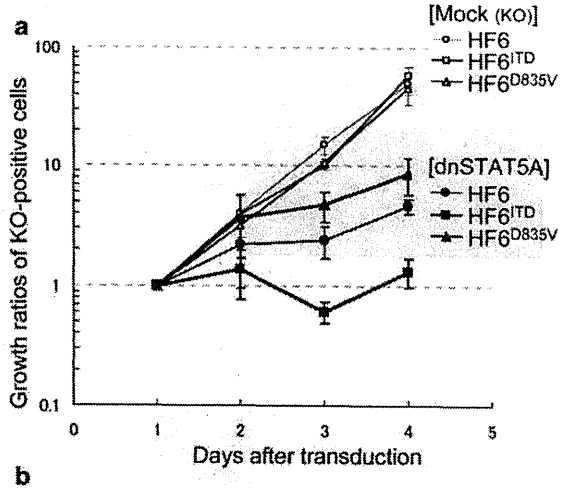
a
[Mock (KO)]
HF6
HF6ITD
HF6D835V
[dnSTAT5A]
HF6
HF6ITD
HF6D835V
Growth ratios of KO-positive cells
Days after transduction

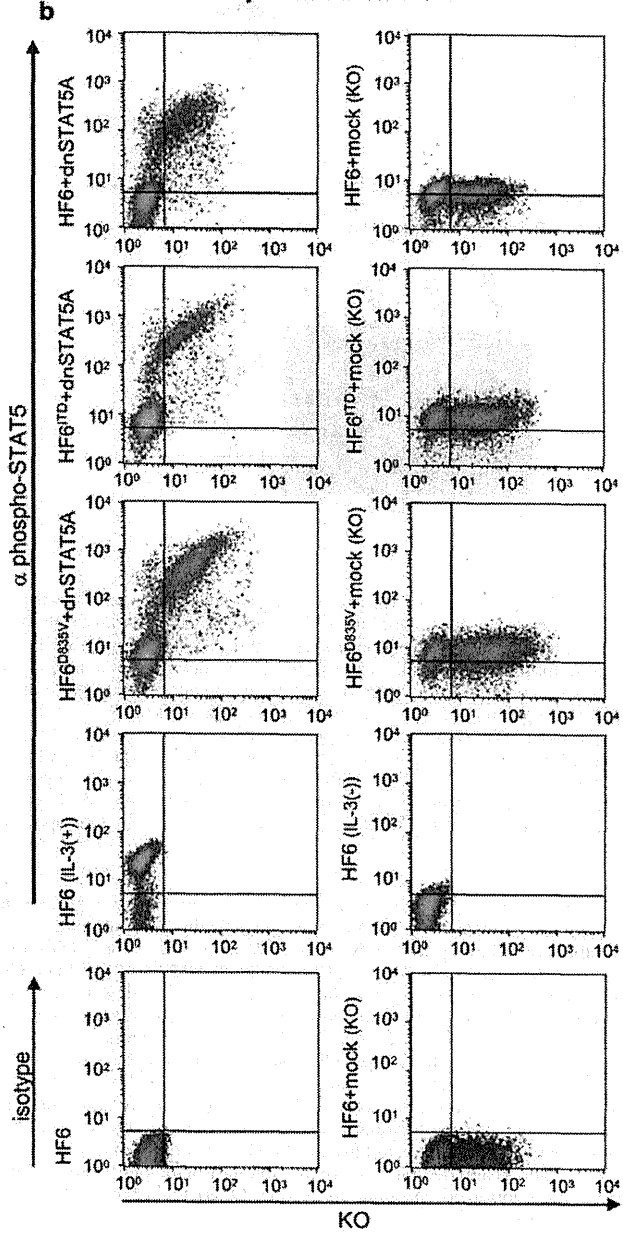
b
α phospho-STAT5
HF6+dnSTAT5A
HF6+mock (KO)
HF6ITD+dnSTAT5A
HF6ITD+mock (KO)
HF6D835V+dnSTAT5A
HF6D835V+mock (KO)
HF6 (IL-3(+))
HF6 (IL-3(-))
isotype
HF6
HF6+mock (KO)
KO

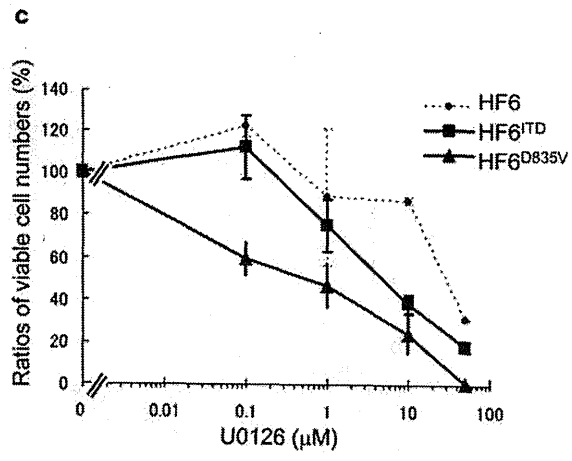
c
HF6
HF6ITD
HF6D835V
Ratios of viable cell numbers (%)
U0126 (μM)

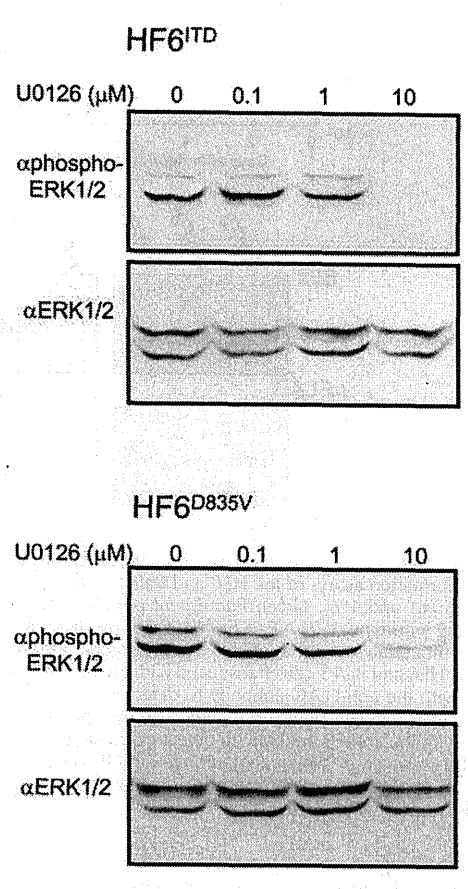
d
HF6ITD
U0126 (μM) 0 0.1 1 10
αphospho-ERK1/2
αERK1/2
HF6D835V
U0126 (μM) 0 0.1 1 10
αphospho-ERK1/2
αERK1/2

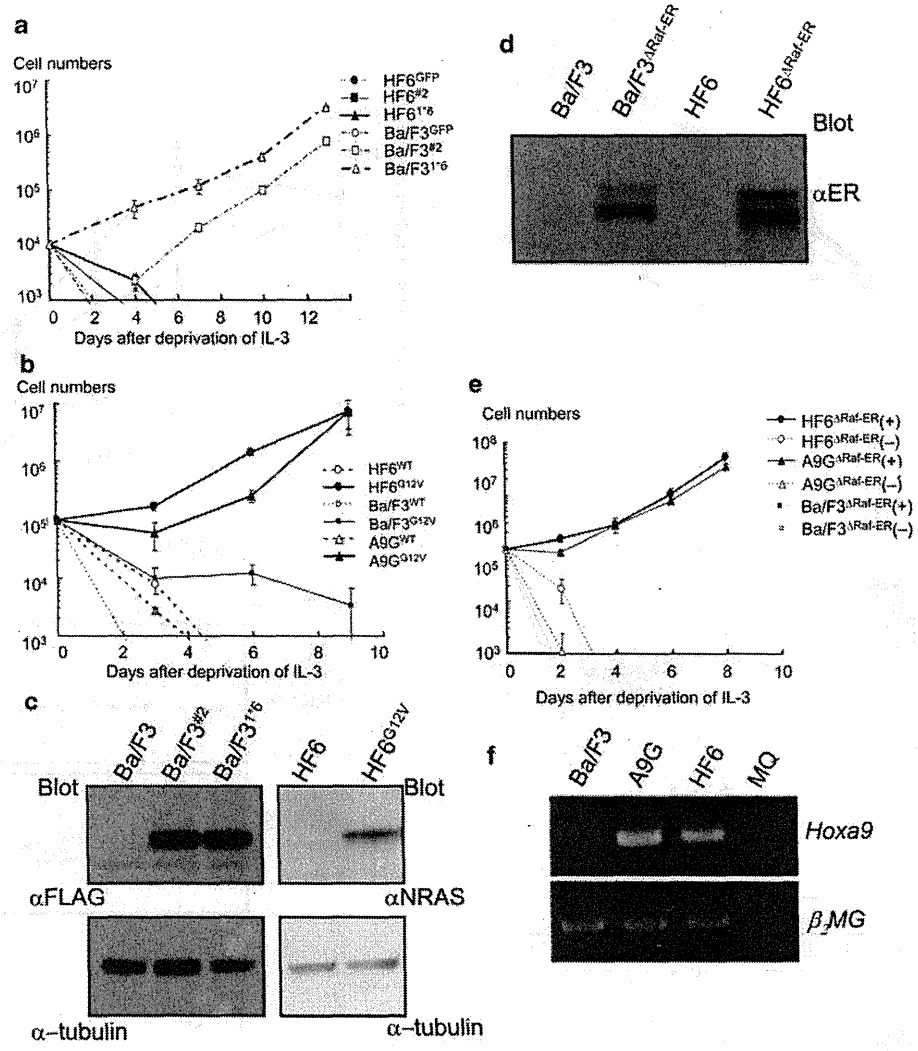

Figure 3 Transformation of the HF6 and A9G cells induced by direct activation of Ras/Raf/mitogen-activated protein kinase (MAPK) pathway. (**a**) Transformation assays of the HF6 and Ba/F3 cells expressing constitutively active forms of signal transducer and activator of transcription 5A (STAT5A) (#2 and 1*6). Green fluorescent protein (GFP) was used as a control. (**b**) Transformation assays of the HF6, A9G and Ba/F3 cells expressing wild-type (WT) *NRAS* or $NRAS^{G12V}$ (G12V). The averages of the number of viable cells with s.d. (bars) are shown in (**a**) and (**b**). (**c**, **d**) Western blot analyses of the whole lysates extracted from the transduced cells (see legends to panels (a) and (b)) in the absence of interleukin-3 (IL-3). (**c**) HF6 and Ba/F3 cells transduced with an inducible form of Raf (Δ*Raf*-estrogen receptor (ER)) (**d**) and their parental cells (**c**, **d**). The blot was probed with the anti-FLAG antibody to detect expression of ectopically expressed STAT5A mutants (upper left panel), or probed with the anti-*NRAS* antibody (upper right panel), followed by reprobe with the anti-α-tubulin antibody as internal control (lower panels) (**c**). The blot was also probed with the anti-ER antibody to detect expression of Δ*Raf*-ER (**d**). (**e**) Transformation assays of the HF6, A9G and Ba/F3 cells expressing Δ*Raf*-ER in the presence of 4-hydroxy-tamoxifen (4-OHT) (+) or vehicle control (–). The averages of the number of viable cells with s.d. (bars) are shown. (**f**) Analysis of *Hoxa9* transcripts in A9G cells using reverse transcriptase-PCR. Ba/F3 and HF6 cells were used as negative and positive controls, respectively.

Figure 4 Leukemogenesis induced by *mixed-lineage-leukemia* (*MLL*)-septin 6 (*SEPT6*) with $NRAS^{G12V}$ synergistically, but not with signal transducer and activator of transcription 5A (STAT5A)#2, *in vivo* under lethal conditioning. (**a**) Survival curves of mice transplanted with *MLL-SEPT6* and $NRAS^{G12V}$ (MS6/G12V; $n=6$), MS6 and *STAT5A*#2 (MS6/#2; $n=6$), MS6/GFP ($n=6$), neo/G12V ($n=6$), neo/#2 ($n=3$) and neo/GFP ($n=3$). (**b**) Representative macroscopic images of spleens obtained from each group of mice shown in (**a**). Scale bar 1 cm. (**c**, **d**) Representative histopathological analysis of morbid mice transplanted with MS6/#2, MS6/G12V (**c**, **d**), neo/G12V, and neo/#2 (**d**). Bone marrow (BM) cells (**c**) and paraffin sections of spleen (**d**) were stained with Wright-Giemsa and hematoxylin and eosin (H&E), respectively. Original magnification, × 200 (**c**) and × 40 (**d**); scale bars, 30 μm (c) and 200 μm (**d**). (**e**, **f**) Immunophenotype of BM or splenic (Sp) cells obtained from representative morbid mice transplanted with MS6/#2 (**e**, left panels), MS6/G12V (**e**, right panels), neo/G12V (**f**, left panels) and neo/#2 (**f**, right panels). The dot plots show each surface antigen labeled with a corresponding monoclonal antibody versus expression of GFP. Ly5.1, Gr-1, CD11b, Ter119, and c-Kit were labeled with phycoerythrin (PE)-conjugated and allophycocyanin (APC)-conjugated monoclonal antibodies, respectively. (**g**) Southern blot analysis to detect clonality (left panel) and proviral integration (right panel). Genomic DNA extracted from BM cells obtained from representative mice transplanted with MS6/G12V (lanes 4, 5, 9 and 10), MS6/GFP (lanes 2, 3, 7 and 8) and neo/GFP (5 months after transplantation; lanes 1 and 6) was digested with *Bam*HI (lanes 1–5) and *Nhe*I (lanes 6–10), respectively, and hybridized with the Neo probe. Oligoclonal bands of proviral integration and single bands of the proviral DNA are indicated by arrows and arrowheads, respectively.

(A9G$^{\Delta Raf-ER}$) cells grew without IL-3 only in the presence of 4-hydroxy-tamoxifen (Figure 3e). Expression level of *Hoxa9* in A9G cells was shown in comparison with those in Ba/F3 and HF6 (negative and positive controls, respectively) cells by reverse transcriptase-PCR (Figure 3f).

Taken together, these results *in vitro* suggested the essential role of activation of the Ras/Raf/MAPK cascade together with *Hoxa9* upregulated by *MLL* fusion proteins in the transformation of the cells expressing *MLL* fusion protein.